CHEMISTRY
A EUROPEAN JOURNAL

DOI: 10.1002/chem.200900904

Understanding, Controlling and Programming Cooperativity in Self-Assembled Polynuclear Complexes in Solution

Thomas Riis-Johannessen,*[a] Natalia Dalla Favera,[a] Tanya K. Todorova,[b] Stefan M. Huber,[b] Laura Gagliardi,[b] and Claude Piguet*[a]

Dedicated to Professor Jean-Claude Bünzli on the occasion of his 65th birthday

Abstract: Deviations from statistical binding, that is cooperativity, in self-assembled polynuclear complexes partly result from intermetallic interactions $\Delta E^{M,M}$, whose magnitudes in solution depend on a balance between electrostatic repulsion and solvation energies. These two factors have been reconciled in a simple point-charge model, which suggests severe and counter-intuitive deviations from predictions based solely on the Coulomb law when considering the variation of $\Delta E^{M,M}$ with metallic charge and intermetallic separation in linear polynuclear helicates. To demonstrate this intriguing behaviour, the ten microscopic interactions that define the thermodynamic formation constants of some twenty-nine homometallic and heterometallic polynuclear triple-stranded helicates obtained from the coordination of the segmental ligands **L1**–**L11** with Zn^{2+} (a spherical d-block cation) and Lu^{3+} (a spherical 4f-block cation), have been extracted by using the site binding model. As predicted, but in contrast with the simplistic coulombic approach, the apparent intramolecular intermetallic interactions in solution are found to be i) more repulsive at long distance ($\Delta E_{1-4}^{Lu,Lu} > \Delta E_{1-2}^{Lu,Lu}$), ii) of larger magnitude when Zn^{2+} replaces Lu^{3+} ($\Delta E_{1-2}^{Zn,Lu} > \Delta E_{1-2}^{Lu,Lu}$) and iii) attractive between two triply charged cations held at some specific distance ($\Delta E_{1-3}^{Lu,Lu} < 0$). The consequences of these trends are discussed for the design of polynuclear complexes in solution.

Keywords: cooperativity · polynuclear complexes · self-assembly · solvation · thermodynamics

Introduction and Theory

In both living[1] and inanimate[2] macroscopic systems, the multi-component assembly of basic subunits plays a crucial role in the design of intelligent organisations and functions. The replication of this approach at the molecular level is at the origin of supramolecular chemistry,[3] an aspect of chemistry which focuses on the combination of molecular building blocks (sometimes called synthons in organic synthesis, tectons in solid-state synthesis, ligands and metal ions in coordination chemistry etc.) to give complex and functional nanoscopic architectures.[4] However, the manipulation and cohesion of molecular units implies changes in both entropic and enthalpic contributions that are much less intuitive than the related purely enthalpic changes accompanying mechanical processes at the macroscopic level. Consequently, the use of thermodynamic equilibria minimizing the Gibbs free energy in solution has become a very popular strategy for controlling the self-assembly process.[5] In 2003, Ercolani[6] elegantly showed that the free energy change accompanying the two-component assembly of *pm* A mole-

[a] Dr. T. Riis-Johannessen,[+] N. Dalla Favera, Prof. Dr. C. Piguet
Department of Inorganic, Analytical and Applied Chemistry
University of Geneva
30 quai E. Ansermet, 1211 Geneva 4 (Switzerland)
Fax: (+41) 22-379-6830
E-mail: thomas.riis-johannessen@epfl.ch
Claude.Piguet@unige.ch

[b] Dr. T. K. Todorova, Dr. S. M. Huber, Prof. Dr. L. Gagliardi
Department of Physical Chemistry
University of Geneva
30 quai E. Ansermet, 1211 Geneva 4 (Switzerland)

[+] Current address:
Swiss Federal Institute of Technology Lausanne (EPFL)
1015 Lausanne (Switzerland)

Supporting information for this article (schematic structures, symmetries and statistical factors for complexes used in multiple non-linear least squares fits (Figure S1–S3); Born–Haber cycles for the successive complexations of Lu^{3+} to *tc*-$[Lu_2(\mathbf{L11})_3]^{6+}$ (Figure S4); calculations of the statistical factors for all complexes used in multiple non-linear least squares fits (Appendix 1); Equations S1–S25 (Appendix 2); full derivation of Equation (49) (Appendix 3); full derivations of Equations (54) and (55) (Appendix 4)) is available on the WWW under http://dx.doi.org/10.1002/chem.200900904.

cules with *pn* B molecules, having *n* and *m* binding sites, respectively, to give the saturated assembly $A_{pm}B_{pn}$ [equilibrium (1)] is simply given by Equation (2) (*m* and *n* are the stoichiometric coefficients and *p* is the complexity[7] of the assembly).

$$pm\,A + pn\,B \rightleftharpoons A_{pm}B_{pn} \quad \Delta G^{0\,A,B}_{pm,pn} = -RT\ln(\beta^{A,B}_{pm,pn}) \tag{1}$$

$$\Delta G^{0\,A,B}_{pm,pn} = -RT\ln(\omega^{A,B}_{pm,pn}) - (pn+pm-1)RT\ln\left(f^{A,B}_{inter}\right) \\ -(pmn-(pn+pm-1))RT\ln\left(f^{A,B}_{intra}\right) \tag{2}$$

The first term corresponds to the symmetry factor of the self-assembly equilibrium and it accounts for the pure entropic driving forces which result primarily from statistics. It can be easily calculated on the basis of symmetry numbers or by a direct counting method providing that the structures and geometries of A, B and $A_{pm}B_{pn}$ are at hand.[8] Following the well-accepted principle of maximum site occupancy,[9] *pm* molecules of A possessing *n* binding sites and *pn* molecules of B possessing *m* binding sites are joined by *pmn* bonds in the final assembly $A_{pm}B_{pn}$. Amongst these, *pm*+*pn*−1 are intermolecular, while the remaining *pmn*−(*pm*+*pn*−1) are intramolecular bonds.[6] The assignment of absolute affinities of $f^{A,B}_{inter}$ and $f^{A,B}_{intra}$ to each specific connecting mode leads to the last two terms of Equation (2). Since only the stability constants $\beta^{A,B}_{pm,pn}$ of the assembly processes are easily accessible in chemistry, Equation (2) transforms into Equation (3) by using the standard vant'Hoff isotherm ($\Delta G^0 = -RT\ln\beta$).[10]

$$\beta^{A,B}_{pm,pn} = \omega^{A,B}_{pm,pn}\left(f^{A,B}_{inter}\right)^{pn+pm-1}\left(f^{A,B}_{intra}\right)^{pmn-pn-pm+1} \tag{3}$$

Subsequent introduction of the so-called concept of effective concentration $c^{eff} = e^{-\left(\Delta H^{A,B}_{intra}-\Delta H^{A,B}_{inter}\right)/RT}e^{\left(\Delta S^{A,B}_{intra}-\Delta S^{A,B}_{inter}\right)/R}$ for correcting the difference in enthalpic and entropic contributions when the intermolecular connection is replaced by its intramolecular counterpart ($f^{A,B}_{intra} = c^{eff}f^{A,B}_{inter}$),[11] eventually gives Equation (4), which applies to any two-component assembly process.[6]

$$\beta^{A,B}_{pm,pn} = \omega^{A,B}_{pm,pn}\left(f^{A,B}_{inter}\right)^{pmn}\left(c^{eff}\right)^{pmn-pn-pm+1} \tag{4}$$

Since the statistical factors $\omega^{A,B}_{pm,pn}$ are not amenable to chemical manipulation, it is obvious that the maximum stability of a given $A_{pm}B_{pn}$ assembly results from the simultaneous optimization of i) $f^{A,B}_{inter}$ via the stereoelectronic matching of the complementary binding units in A and B,[12] and ii) c^{eff} via structural preorganisation favoring intra- over intermolecular connections.[13] When both $f^{A,B}_{inter}$ and c^{eff} parameters are constant for all connections in $A_{pm}B_{pn}$, the self-assembly process is said to be statistical or non-cooperative.[6] Any variation of c^{eff} is assigned to changes in *preorganisation* occurring within the self-assembly process, while related changes of $f^{A,B}_{inter}$ are assigned to *cooperativity*, which can be either positive ($f^{A,B}_{inter}$ increases) or negative ($f^{A,B}_{inter}$ decreases). The 'sign' (i.e. positive or negative) of cooperativity for purely intermolecular assembly processes ($m=1$ or $n=1$) can be easily deduced from evaluation of the classical Langmuir isotherm[14] or from the construction of well-known Scatchard or Hill plots,[15] whilst Hamacek plots are required when both inter- and intramolecular processes operate concurrently.[16] According to the Ising model,[17] the apparent variation of $f^{A,B}_{inter}$ in cooperative processes can be attributed to the neglect of the homo-component interactions $\Delta E^{A,A}$ and $\Delta E^{B,B}$ operating in the final assembly. Their introduction as correcting Boltzmann factors in Equation (4) leads to the extended site binding model [Eq. (5)],[18] in which deviations from statistics can be explicitly assigned to specific homo-component interactions.[9c,d]

$$\beta^{A,B}_{pm,pn} = \omega^{A,B}_{pm,pn}\left(f^{A,B}_{inter}\right)^{pmn}\left(c^{eff}\right)^{pmn-pn-pm+1}\prod_i e^{-\Delta E^{A,A}_i/RT}\prod_j e^{-\Delta E^{B,B}_j/RT} \tag{5}$$

For sterically unencumbered and neutral A and B components, we predict that the additional homo-component interactions are much weaker than the targeted intercomponent connections (i.e. $|\Delta E^{A,A}| \approx |\Delta E^{B,B}| \ll |\Delta E^{A,B}| = |-RT\ln(f^{A,B}_{inter})|$), which explains the rarity of strongly cooperative processes in synthetic supramolecular assemblies.[16,19] However, chemical intuition also suggests that the situation could be rather different when charged components are involved, and the complexation of metallic cations with neutral ligands thus represents an ideal target process for rationalizing and exploiting cooperativity [Eq. (6)].

$$m\,M^{z+} + n\,L \rightleftharpoons [M_mL_n]^{mz+} \quad \Delta G^{0\,M,L}_{m,n} = -RT\ln(\beta^{M,L}_{m,n}) \tag{6}$$

The original analysis of the self-assembly of Lehn's famous double-stranded helicates $[Cu_3(\mathbf{L12})_3]^{3+}$ (Figure 1a)[20] with Equations (3) and (4) by Ercolani indeed showed negligible deviations from statistics.[6] Later though, thorough treatment of all available thermodynamic data for this system with Equation (5) concluded that a modest but average negative cooperativity characterised the successive fixation of both ligands ($\Delta E^{L12,L12} = 4(2)\ kJ\,mol^{-1}$) and Cu^I ions in solution ($\Delta E^{Cu,Cu}_{1-2} = 5(3)\ kJ\,mol^{-1}$, the subscripted 1-2 index indicating a geminal intermetallic interaction between two cations in neighboring sites).[9d] If the interligand interaction is rather difficult to rationalize because of the contributions from steric crowding and metal polarization effects, the intermetallic interaction should rely on electrostatic interactions, which can be roughly modeled with Coulomb Equation (7) assuming that the metal ions are considered as non-polarizable point charges (N_A is Avogadro's number = $6.023\times10^{23}\ mol^{-1}$, z_i are the charges of the interacting particles in electrostatic units, e is the elemental charge = 1.602×10^{-19} C, ε_0 is the dielectric constant of vacuum = $8.859\times10^{-12}\ C^2N^{-1}m^{-2}$, ε_r is the relative dielectric permittivity of the medium and d is the intermetallic separation). Assuming that the dominant local dielectric constant operating at short distance in the final supramolecular complex is close to that of vacuum ($\varepsilon_r \approx 1$),[21,22] we calculate $\Delta E^{Cu,Cu}_{1-2,calcd} =$

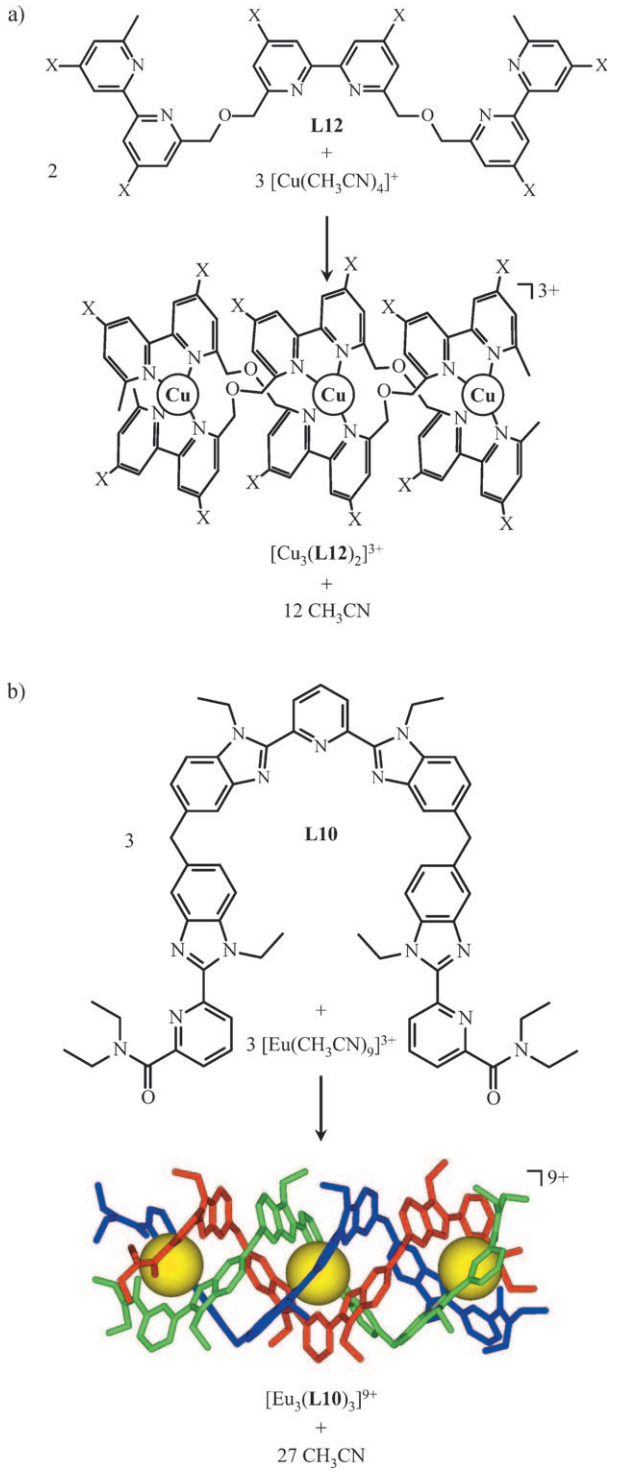

Figure 1. Self-assembly of cationic a) double-stranded $[Cu_3(\mathbf{L12})_2]^{3+}$ (X = CO_2Et)[20] and (b) triple-stranded $[Eu_3(\mathbf{L10})_3]^{9+}$ helicates.[33]

239 kJ mol^{-1} for two Cu^{I} ions separated by 5.8 Å in $[Cu_3(\mathbf{L12})_3]^{3+}$.

$$\Delta E^{M,M}_{calcd} = -\frac{z_1 z_2 e^2 N_A}{4\pi\varepsilon_0}\int_{\infty}^{d}\frac{dr}{\varepsilon_r r^2} = \frac{z_1 z_2 e^2 N_A}{4\pi\varepsilon_0\varepsilon_r d} \quad (7)$$

The discrepancy is even more striking for the related assembly processes leading to the triple-stranded lanthanide helicate $[Eu_3(\mathbf{L10})_3]^{9+}$ (Figure 1b), for which the experimental value measured in acetonitrile $\Delta E^{Eu,Eu}_{1-2} = 8(4)$ kJ mol^{-1} [21] has no relationship whatsoever with $\Delta E^{Eu,Eu}_{1-2,calcd} = 1389$ kJ mol^{-1}, obtained with Equation (7) for two triply charged cations held at about 9.0 Å. The origin of the drastic reduction in intermetallic interactions in solution, which ensures a reasonable stability for these highly charged helicates, has been tentatively assigned to a compensation of the electrostatic repulsion by the increase in solvation energy associated with the accumulation of charge in the final complex.[22] If we roughly model the solvation energies of the charged complexes with Born Equation (8) (R is the pseudo-spherical radius of the charged ion in a non-constrained phase, i.e. solution or gas-phase),[23] it becomes apparent that the magnitudes of the intermetallic interactions, which operate during the assembly of charged complexes in solution, deviate from the intuitive $z_1 z_2/d$ dependence anticipated from sole consideration of the Coulomb law.

$$\Delta_{solv}G^0 = -\frac{z^2 e^2 N_A}{8\pi\varepsilon_0 R}\left(1-\frac{1}{\varepsilon_r}\right) \quad (8)$$

Recently, we reported on the structural and thermodynamic investigations of the first directional triple-stranded heterometallic helicate *HHH*-$[Lu_2Zn(\mathbf{L1})_3]^{8+}$, based on segmental pyridyl-benzimidazole ligand **L1** (Scheme 1).[24] The mere preparation of this complex is perhaps not overwhelmingly noteworthy in its own right, given the now widespread appreciation for the importance of stereoelectronic matching between metal ion and ligand binding site in metallosupramolecular design, but its detailed thermodynamic investigation has presented an opportunity to address previously inaccessible intermetallic interactions in solution. The complex features a linear arrangement of two Lu^{3+} trications and one Zn^{2+} dication, separated by regular intervals of about 9 Å. Reflected in its cumulative formation constant, therefore, are not only contributions from the above-mentioned geminally interacting lanthanide trications, but also geminal (1-2) and vicinal (1-3, ca. 18 Å) interactions operating between the Zn^{2+} and Lu^{3+} di- and trications. In this contribution, we thus combine the thermodynamic data reported for *HHH*-$[Lu_2Zn(\mathbf{L1})_3]^{8+}$,[24] with that collected during the last decade for a series of closely related homo- and heterometallic complexes based on ligands **L2**,[25] **L3**,[26] **L4**,[27] **L5**,[28] **L6**,[29] **L7**,[30] **L8**,[22,31] **L9**,[32] **L10**[33] and **L11**[21] (Scheme 1), to obtain a reliable set of ten microscopic thermodynamic parameters for describing the principal interactions operating during their self-assembly. This detailed analysis brings to light a number of important considerations for programming multi-component assemblies, amongst which are the various contributions to cooperativity. Finally, focusing exclusively on the cation–cation interactions, we propose a simple predictive model for estimating $\Delta E^{M,M}$ and its dependence on both intermetallic separation and metallic charge in linear self-assembled complexes in solution.

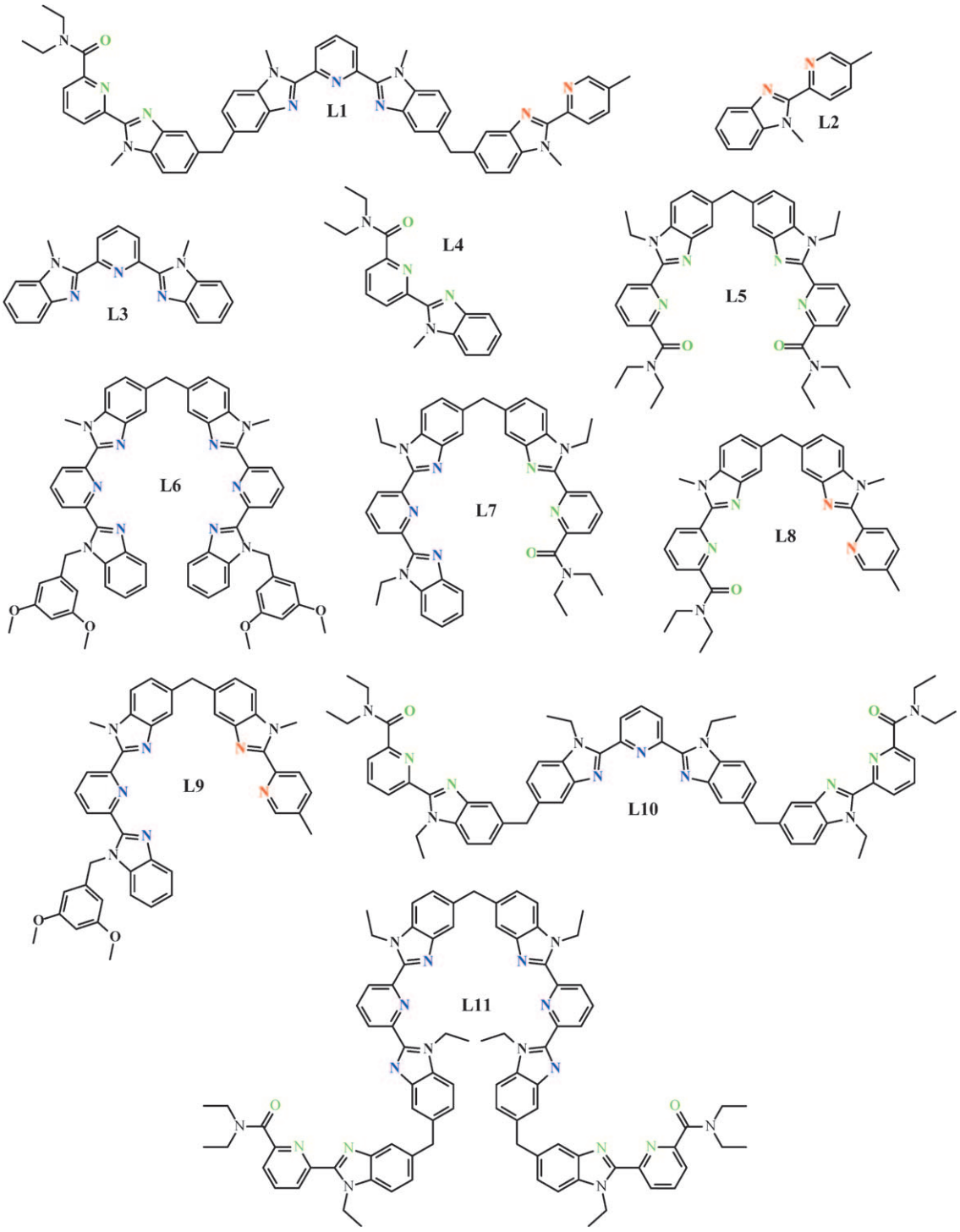

Scheme 1. Structures of the ligands **L1**–**L11** highlighting tridentate N_3 (blue), N_2O (green) and bidente N_2 (red) binding sites.

Results and Discussion

Extracting microscopic thermodynamic parameters: The segmental ligands **L1**–**L11** strictly match the following criteria: i) they contain a repertoire of only three different semi-planar aromatic binding units, that is two tridentate N_3 and N_2O chelating units and one bidentate N_2 chelating unit, and ii) each pair of chelating segment is linked by a diphenylmethane spacer, which holds two adjacent metals at 8.86–9.41 (ca. 9) Å in the resulting helicates.[21,22,28,29] Moreover, only complexes with the tridentate units bound to Lu^{3+} and the bidentate site bound to Zn^{2+} are considered

for the global thermodynamic analysis. Within these boundary conditions, the application of the extended site binding model[9c,d] to describe the cumulative stability constants of complexes based on such polytopic ligands requires some minor adaptations from the simplified form expressed in Equation (5). The convention adopted from henceforth for the assembly of generic complex $\left[Lu_{m_1}Zn_{m_2}(\mathbf{L}\phi)_n\right]^{(3m_1+2m_2)+}$ [Equilibrium (9)] is summarised in Equation (10), where m_1 and m_2 represent the stoichiometric coefficients of the Lu^{3+} and Zn^{2+} ions and n is the stoichiometric coefficient of the ligand $\mathbf{L}\phi$. Given that all one-dimensional helicates are of first-order complexity, the coefficient p is set to 1 and can thus be neglected.

$$m_1\,Lu^{3+} + m_2\,Zn^{2+} + n\,\mathbf{L}\phi \rightleftharpoons \left[Lu_{m_1}Zn_{m_2}(\mathbf{L}\phi)_n\right]^{(3m_1+2m_2)+} \quad (9)$$

$$\begin{aligned}\beta^{Lu,Zn,\mathbf{L}\phi}_{m_1,m_2,n} &= e^{-\left(\Delta G^{Lu,Zn,\mathbf{L}\phi}_{m_1,m_2,n}/RT\right)}\\ &= \omega^{Lu,Zn,\mathbf{L}\phi}_{m_1,m_2,n}\prod_{i=1}^{m_1 n}\left(f^{Lu}_{N_2O/N_3}\right)\prod_{i=1}^{m_2 n}\left(f^{Zn}_{N_2}\right)^{(m_1+m_2)n-m_1-m_2-n+1}\prod_{i=1}\\ &(c^{eff})\prod_{i<j}\left(u^{Lu,Lu}_{ij}\right)\prod_{h<k}\left(u^{Zn,Lu}_{hk}\right)\prod_{p<q}\left(u^{L,L}_{pq}\right)\end{aligned} \quad (10)$$

In this equation, the factor $\omega^{Lu,Zn,\mathbf{L}\phi}_{m_1,m_2,n}$ has its usual meaning and takes into account the statistical entropy changes inherent to the equilibrium in question.[8] The second term from Equation (5), $f^{A,B}_{inter}$, has been separated into three metal specific terms, $f^{Lu}_{N_2O}$, $f^{Lu}_{N_3}$ and $f^{Zn}_{N_2}$, each accounting for the microscopic affinities of Lu^{3+} and Zn^{2+} for tridentate (N_2O/N_3) and bidentate (N_2) sites respectively. The term describing homo-component interactions between charged cations has likewise been separated into two Boltzmann factors, $u^{Lu,Lu}_{ij} = e^{-\left(\Delta E^{Lu,Lu}_{ij}/RT\right)}$ and $u^{Zn,Lu}_{hk} = e^{-\left(\Delta E^{Zn,Lu}_{hk}/RT\right)}$, each accounting for the respective interactions between like ($Lu^{3+}\cdots Lu^{3+}$) and unlike ($Zn^{2+}\cdots Lu^{3+}$) cation pairs in the bimetallic complexes at various distances (ij=1-2 for a geminal intraction at 9 Å, ij=1-3 for a vicinal intraction at 18 Å and ij=1-4 for a distal intraction at 27 Å). Finally, the second homo-component term, $u^{L,L}_{pq} = e^{-\left(\Delta E^{L,L}_{pq}/RT\right)}$, which accounts for the interaction between any two binding sites complexed to a common metal ion, is set to include all possible combinations of inter-ligand interaction (i.e. the condition $u^{L,L}_{tri-,tri-} = u^{L,L}_{bi-,bi-} = u^{L,L}_{bi-,tri-} = u^{L,L}$ complies). Granting the two standard assumptions pertinent to helicate assemblies based on semi-rigid ligands that i) no hairpin or strained structures are formed and ii) the principle of maximum site-occupancy prevails,[9c,d] application of Equation (10) to, for example, the Equilibrium (11) leading to the recently reported bimetallic trinuclear complex HHH-$[Lu_2Zn(\mathbf{L1})_3]^{8+}$[24] gives the corresponding Equation (12).

$$3\,\mathbf{L1} + 2\,Lu^{3+} + Zn^{2+} \rightleftharpoons [Lu_2Zn(\mathbf{L1})_3]^{8+} \quad \log\beta^{Lu,Zn,\mathbf{L1}}_{2,1,3} = 36(1) \quad (11)$$

$$\begin{aligned}\beta^{Lu,Zn,\mathbf{L1}}_{2,1,3} &= \beta^{Lu,Zn,\mathbf{L1}}_{2,1,3}(HHH)\\ &= 576\left(f^{Lu}_{N_2O}\right)^3\left(f^{Lu}_{N_3}\right)^3\left(f^{Zn}_{N_2}\right)^3(c^{eff})^4\left(u^{Zn,Lu}_{1-2}\right)\left(u^{Zn,Lu}_{1-3}\right)\left(u^{Lu,Lu}_{1-2}\right)\left(u^{L,L}\right)^9\end{aligned} \quad (12)$$

The statistical factor $\omega^{Lu,Zn,\mathbf{L1}}_{2,1,3}=576$ has been evaluated by using the symmetry number method originally proposed by Benson [Eq. (14) and Figure 2].[34] It is given by the ratio between the product of the symmetry numbers of the reactants and that of the product species, each taken to the power of their stoichiometric coefficients. Symmetry numbers for the individual components are in turn given by the product of i) an external symmetry factor, σ^{ext}, which accounts for the various different but undistinguishable atomic arrangements incurred by rotating the molecule as a whole about first-order symmetry elements and ii) an internal symmetry factor, σ^{int}, which takes the same definition, but accounts for different atomic arrangements achieved exclusively by internal rotations about freely rotatable C–C single or metal–ligand coordination bonds. These are further multiplied by a third factor, σ^{chi}, if one or more of the participants is chiral and present at equilibrium as a racemic mixture, since this gives rise to an equal quantity of two opposite enantiomers with identical symmetries. The latter equates to $\sigma^{chi}={}^1/_2$ for an unresolved chiral species, such as the C_3-symmetrical helicate HHH-$[Lu_2Zn(\mathbf{L1})_3]^{8+}$, and $\sigma^{chi}=1$ when the species formed is achiral.[8]

Application of these criteria to the evaluation of a statistical factor $\omega^{Lu,Zn,\mathbf{L1}}_{2,1,3}$ for the formation of the bimetallic helicate HHH-$[Lu_2Zn(\mathbf{L1})_3]^{8+}$ in Equation (11) is exemplified below. To maintain a complete picture of the equilibrium in question, solvent molecules (MeCN) from the first coordination sphere have also been included. Equilibrium (11) may thus be written as Equation (13), which, now that it considers i) free Lu^{3+} as a D_{3h} symmetric tricapped trigonal prismatic complex $[Lu(MeCN)_9]^{3+}$[35] and ii) free Zn^{2+} as an octahedral complex $[Zn(MeCN)_6]^{2+}$, takes into account any

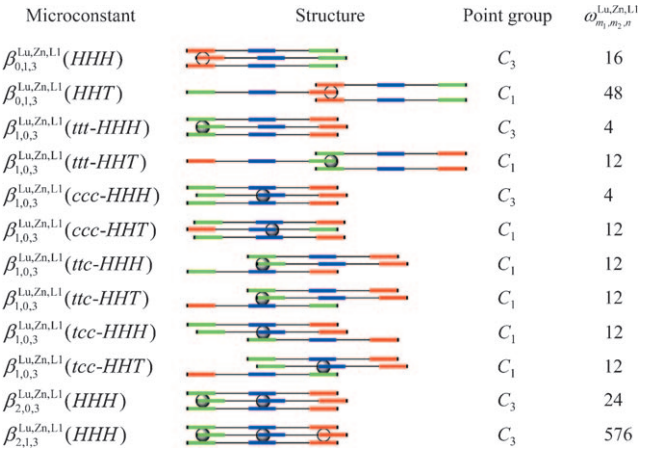

Figure 2. Schematic structures showing tridentate N_2O (green), N_3 (blue) and bidentate N_2 (red) binding sites, symmetries and statistical factors for $[Lu_{m_1}Zn_{m_2}(\mathbf{L1})_3]^{(3m_1+2m_2)+}$ (m_1=0–2; m_2=0, 1) microspecies. Shaded and empty circles represent Lu^{3+} and Zn^{2+} ions respectively.

changes in rotational and translational entropy associated with the liberation of solvent molecules from the metal ions.

$$3\,\mathbf{L1} + 2\,[Lu(MeCN)_9]^{3+} + [Zn(MeCN)_6]^{2+} \rightleftharpoons [Lu_2Zn(\mathbf{L1})_3]^{8+} + 24\,MeCN \quad (13)$$

Symmetry	C_s	D_{3h}	O_h	C_3	C_{3v}
σ^{ext}	1	6	24	3	3
σ^{int}	1	3^9	3^6	1	1
σ^{chi}	1	1	1	1/2	1

$$\omega_{2,1,3}^{Lu,Zn,\mathbf{L1}} = \frac{(\sigma_{Lu(MeCN)_9})^2(\sigma_{Zn(MeCN)_6})(\sigma_{\mathbf{L1}})^3}{(\sigma_{Lu_2Zn(\mathbf{L1})_3})(\sigma_{MeCN})^{24}} = \frac{(6\cdot 3^9\cdot 1)^2\cdot(24\cdot 3^6\cdot 1)\cdot(1\cdot 1\cdot 1)^3}{(3\cdot 1\cdot 1/2)\cdot(3\cdot 1\cdot 1)^{24}} = 576 \quad (14)$$

As is often the case for this type of system, a number of other (homometallic) species were also identified as key intermediates in the self-assembly of *HHH*-$[Lu_2Zn(\mathbf{L1})_3]^{8+}$.[24] Within the precincts of the criteria discussed above, similar treatment for these Equilibria (15), (17) and (19) thus gives a corresponding set of Equations (16), (18) and (20) (Figure 2). Note that apart from the stoichiometries inferred from ESI-MS and UV/Vis titrations, very little structural information is available for the intermediate species $[Zn(\mathbf{L1})_3]^{2+}$ and $[Lu(\mathbf{L1})_3]^{3+}$,[24] and their cumulative macroscopic stability constants are modelled by the sum of the microscopic formation constants characterising the different conceivable structural isomers (or microspecies) present at equilibrium (Figure 2 and Appendix I in the Supporting Information).[9c,d] Indeed, only for the saturated complexes *HHH*-$[Lu_2(\mathbf{L1})_3]^{6+}$ and *HHH*-$[Lu_2Zn(\mathbf{L1})_3]^{8+}$ do the cumulative formation constants equate to a single microconstant since these complexes are the only species present in significant quantity at equilibrium for their corresponding stoichiometries.[24]

$$3\,\mathbf{L1} + Zn^{2+} \rightleftharpoons [Zn(\mathbf{L1})_3]^{2+} \quad \log\beta_{0,1,3}^{Lu,Zn,\mathbf{L1}} = 22.3(5) \quad (15)$$

$$\beta_{0,1,3}^{Lu,Zn,\mathbf{L1}} = \beta_{0,1,3}^{Lu,Zn,\mathbf{L1}}(HHH) + \beta_{0,1,3}^{Lu,Zn,\mathbf{L1}}(HHT) = 64\left(f_{N_2}^{Zn}\right)^3\left(u^{L,L}\right)^3 \quad (16)$$

$$3\,\mathbf{L1} + Lu^{3+} \rightleftharpoons [Lu(\mathbf{L1})_3]^{3+} \quad \log\beta_{1,0,3}^{Lu,Zn,\mathbf{L1}} = 16.7(2) \quad (17)$$

$$\begin{aligned}\beta_{1,0,3}^{Lu,Zn,\mathbf{L1}} &= \beta_{1,0,3}^{Lu,Zn,\mathbf{L1}}(ttt-HHH) + \beta_{1,0,3}^{Lu,Zn,\mathbf{L1}}(ttt-HHT)\\ &+\beta_{1,0,3}^{Lu,Zn,\mathbf{L1}}(ccc-HHH) + \beta_{1,0,3}^{Lu,Zn,\mathbf{L1}}(ccc-HHT)\\ &+\beta_{1,0,3}^{Lu,Zn,\mathbf{L1}}(ttc-HHH) + \beta_{1,0,3}^{Lu,Zn,\mathbf{L1}}(ttc-HHT)\\ &+\beta_{1,0,3}^{Lu,Zn,\mathbf{L1}}(tcc-HHH) + \beta_{1,0,3}^{Lu,Zn,\mathbf{L1}}(tcc-HHT)\\ &= 16\left(f_{N_2O}^{Lu}\right)^3\left(u^{L,L}\right)^3 + 16\left(f_{N_3}^{Lu}\right)^3\left(u^{L,L}\right)^3 + 24\left(f_{N_2O}^{Lu}\right)^2\left(f_{N_3}^{Lu}\right)\left(u^{L,L}\right)^3\\ &+24\left(f_{N_2O}^{Lu}\right)\left(f_{N_3}^{Lu}\right)^2\left(u^{L,L}\right)^3\end{aligned} \quad (18)$$

$$3\,\mathbf{L1} + 2\,Lu^{3+} \rightleftharpoons HHH\text{-}[Lu_2(\mathbf{L1})_3]^{6+} \quad \log\beta_{2,0,3}^{Lu,Zn,\mathbf{L1}} = 24.2(3) \quad (19)$$

$$\beta_{2,0,3}^{Lu,Zn,\mathbf{L1}} = \beta_{2,0,3}^{Lu,Zn,\mathbf{L1}}(HHH) = 24\left(f_{N_2O}^{Lu}\right)^3\left(f_{N_3}^{Lu}\right)^3\left(c^{eff}\right)^2\left(u_{1-2}^{Lu,Lu}\right)\left(u^{L,L}\right)^6 \quad (20)$$

Equations (12), (16), (18) and (20) constitute a rigorous mathematical description of the formation constants leading to the homo- (Lu^{3+} *or* Zn^{2+}) and bimetallic (Lu^{3+} *and* Zn^{2+}) complexes of **L1**. It is clear, however, that the four experimental $\log\beta_{m_1,m_2,n}^{Lu,Zn,\mathbf{L1}}$ values associated with Equilibria (11), (15), (17) and (19) are insufficient to reliably fit the eight microscopic thermodynamic parameters ($f_{N_2O}^{Lu}$, $f_{N_3}^{Lu}$, $f_{N_2}^{Zn}$, c^{eff}, $u^{L,L}$, $u_{1-2}^{Zn,Lu}$, $u_{1-3}^{Zn,Lu}$, $u_{1-2}^{Lu,Lu}$) included as variables. We have therefore combined the thermodynamic data recently obtained for the above equilibria[24] with that previously reported for i) the mononuclear complexes of bidentate **L2**[24] and tridentate ligands **L3**,[26] **L4**,[27] **L5**[28] and **L8**,[31] ii) the binuclear complexes of **L5**,[28] **L6**[29] and **L7**,[30] iii) the binuclear bimetallic complexes of **L8**[31] and **L9**,[32] and iv) the tri- and tetranuclear Lu^{3+} complexes of **L10**[33] and **L11**[21] (see Appendix 1 and Figure S1–S3 for statistical factors and schematic structures, Supporting Information). This now provides 25 supplementary $\log\beta_{m_1,m_2,n}^{Lu,Zn,\mathbf{L}\phi}$ values and their corresponding equations (Eqs. S1–S25 in Appendix 2 in the Supporting Information) at the expense of the introduction of only two more variables; namely, the long-distance vicinal (1-3) and distal (1-4) intermetallic interactions, $u_{1-3}^{Lu,Lu}$ and $u_{1-4}^{Lu,Lu}$, operating between two Lu^{3+} trications separated by three (ca. 18 Å) and four (ca. 27 Å) binding sites, respectively, in the tri- and tetranuclear helicates based on **L10**[33] and **L11**.[21] Furthermore, the data/parameter ratio of 29/10 = 2.9 is now sufficiently high to justify an attempt at adjusting all ten parameters without imposing constraints on any of the intermetallic interactions, as has previously been required in related investigations.[9(b),21] Indeed, only for the term c^{eff} is it necessary to constrain the dependence on distance so that the condition $c_{1-x}^{eff} = c_{1-2}^{eff}/(x-1)^{\alpha}$ is satisfied, where α takes one of two limiting values, 1.5 or 3, which apply, respectively, if the chain connecting two sites involved in an intramolecular cyclisation is long and highly flexible or of optimised length (both cases are considered herein).[11] It is worth noting here that the theoretical concept of effective concentration is often replaced by the closely related terminology of effective molarity (*EM*), when it is determined experimentally.[5b,e] For the sake of clarity in this contribution, we will use effective concentration for both the theoretical concept and its experimental value for the rest of the discussion.

The simultaneous non-linear least-squares fits of Equations (12), (16), (18), (20) and S1–S25 modelling the formation of complexes $[Lu_{m_1}Zn_{m_2}(\mathbf{L}\phi)_n]^{(3m_1+2m_2)+}$ (ϕ = 1–11; m_1 = 0–4; m_2 = 0–1; n = 1–3) now converge to give the ten microscopic parameters collected in Table 1. Agreement factors (*AF*) lying in the range 0.0003 (α = 3) – 0.0004 (α = 1.5) indicate that the data has been excellently modelled, and the re-

Table 1. Fitted microscopic thermodynamic parameters for $[Lu_{m_1}Zn_{m_2}(\mathbf{L}\phi)_3]^{(3m_1+2m_2)+}$ ($m_1=0$–3; $m_2=0$, 1; $n=1$–3; $\phi=1$–11; simultaneous multi non-linear least-squares fits of Equations (12), (16), (18), (20) and S1–S25 in the Supporting Information; MeCN, 298 K).[a]

Microscopic parameters	$\alpha=1.5$	$\alpha=3$
$\log(f_{N_2O}^{Lu,L\phi})/\Delta g_{N_2O}^{Lu,L\phi}$ [kJ mol^{-1}]	5.4(2)/−31(1)	5.5(2)/−31(1)
$\log(f_{N_3}^{Lu,L\phi})/\Delta g_{N_3}^{Lu,L\phi}$ [kJ mol^{-1}]	5.2(2)/−30(1)	5.3(2)/−30(1)
$\log(f_{N_2}^{Zn,L\phi})/\Delta g_{N_2}^{Zn,L\phi}$ [kJ mol^{-1}]	6.9(3)/−40(1)	7.0(3)/−40(1)
$\log(c^{eff})/\Delta g_{corr}^{M,L\phi}$ [kJ mol^{-1}]	−4.1(4)/23(2)	−3.9(4)/23(2)
$\log(u^{L,L})/\Delta E^{L,L}$ [kJ mol^{-1}]	−0.1(3)/0(2)	−0.1(3)/1(2)
	Solution-phase	Gas-phase[c]
$\log(u_{1-2}^{Lu,Lu})/\Delta E_{1-2}^{Lu,Lu}$ [kJ mol^{-1}]	−0.2(3)/1(2)	−0.6(3)/4(1) 1389[d]
$\log(u_{1-2}^{Zn,Lu})/\Delta E_{1-2}^{Zn,Lu}$ [kJ mol^{-1}]	−2.8(3)/16(2)	−3.1(3)/18(2) 926[e]
$\log(u_{1-3}^{Lu,Lu})/\Delta E_{1-3}^{Lu,Lu}$ [kJ mol^{-1}]	1.1(7)/−6(3)	1.4(7)/−8(3) 695[f]
$\log(u_{1-3}^{Zn,Lu})/\Delta E_{1-3}^{Zn,Lu}$ [kJ mol^{-1}]	0.6(6)/−4(3)	0.8(6)/−4(2) 463[g]
$\log(u_{1-4}^{Lu,Lu})/\Delta E_{1-4}^{Lu,Lu}$ [kJ mol^{-1}]	−3.0(8)/17(5)	−3.2(8)/18(4) 463[h]
AF[b]	0.0004	0.0003

[a] The uncertainties correspond to those obtained during the multi non-linear least-squares fit process. [b] Agreement factor $AF=\sqrt{\left(\sum_i(\log(\beta_i^{exp})-\log(\beta_i^{calcd}))^2\right)/\left(\sum_i(\log(\beta_i^{exp}))^2\right)}$. [c] Calculated with Coulomb Equation (7) considering the metal ions as non-polarizable point charges and using [d] $z_1=z_2=3$; $d=9$ Å, [e] $z_1=3$; $z_2=2$; $d=9$ Å, [f] $z_1=z_2=3$; $d=18$ Å, [g] $z_1=3$; $z_2=2$; $d=18$ Å and [h] $z_1=z_2=3$; $d=27$ Å.

constituted macroscopic cumulative stability constants closely match their experimental counterparts (Table 2, Figure 3). Since the choice of $\alpha=1.5$ or 3 has only minor effect on the resulting parameters (Table 1), further discussions systematically refer to $\alpha=3$.

The microscopic affinities $\Delta g_{N_2O}^{Lu,L\phi}=-31(1)$ and $\Delta g_{N_3}^{Lu,L\phi}=-30(1)$ kJ mol^{-1} describing the intermolecular connections between Lu^{3+} and the tridentate N_2O and N_3 sites (including desolvation) are almost identical to the values $\Delta g_{N_2O}^{Eu,L\phi}=-32(1)$ and $\Delta g_{N_3}^{Eu,L\phi}=-30(1)$ kJ mol^{-1} established from earlier fits based exclusively on the mono- and polynuclear Eu^{3+} complexes of ligands **L5**, **L6**, **L10** and **L11**.[21] The affinity of Zn^{2+} for the bidentate N_2 site appears marginally higher by about 10 kJ mol^{-1} ($\Delta g_{N_2}^{Zn,L\phi}=-40(1)$ kJ mol^{-1}) than Ln^{3+} (Ln = Lu, Eu) for the tridentate sites. This could be a result of stronger metal-ligand orbital interaction between the bidentate N_2 unit and the more expansive 3d, 4s and 4p orbitals on Zn^{2+}. It must be pointed out, however, that the term $\Delta g_{N_2}^{Zn,L\phi}=-40(1)$ reflects a balance between the free energies of bond making (with the entering ligand) and bond breaking (with the liberated solvent molecules) and, as such, an absolute correlation with the nature of the metal–ligand connection is not appropriate.

Table 2. Experimental and calculated[a] cumulative formation constants for complexes $[Lu_{m_1}Zn_{m_2}(\mathbf{L}\phi)_3]^{(3m_1+2m_2)+}$ ($\phi=1$–11; $m_1=0$-4; $m_2=0$–1; $n=1$–3).

Complex	$\log\beta^{calcd}$	$\log\beta^{exp}$	Complex	$\log\beta^{calcd}$	$\log\beta^{exp}$
$[Lu(\mathbf{L1})_3]^{3+}$	17.6	16.7(2)[b,c]	$[Lu_2(\mathbf{L5})_2]^{6+}$	18.8	19.3(4)[c,f]
$[Lu_2(\mathbf{L1})_3]^{6+}$	24.1	24.2(3)[b,c]	$[Lu_2(\mathbf{L6})_3]^{6+}$	24.2	24.3(4)[c,g]
$[Lu_2Zn(\mathbf{L1})_3]^{8+}$	35.8	36(1)[b,c]	$[Lu_2(\mathbf{L7})_3]^{6+}$	24.7	23.9(5)[c,h]
$[Zn(\mathbf{L1})_3]^{2+}$	22.4	22.3(5)[b,c]	$[LuZn(\mathbf{L8})_3]^{5+}$	27.4	28.6(6)[c,i]
$[Zn(\mathbf{L2})]^{2+}$	8.4	7.9(2)[b,c]	$[LuRu(\mathbf{L8})_3]^{5+}$	5.7	5.2(2)[c,j]
$[Zn(\mathbf{L2})_2]^{2+}$	15.8	15.6(3)[b,c]	$[Zn(\mathbf{L8})_3]^{2+}$	22.4	22(1)[c,i]
$[Zn(\mathbf{L2})_3]^{2+}$	22.4	22.7(4)[b,c]	$[LuZn(\mathbf{L9})_3]^{5+}$	26.9	26.2(3)[c,k]
$[Lu(\mathbf{L3})]^{3+}$	6.1	7.4(3)[d]	$[Lu_2(\mathbf{L10})_3]^{6+}$	25.9	26(1)[c,l]
$[Lu(\mathbf{L3})_2]^{3+}$	11.6	13.1(4)[d]	$[Lu_3(\mathbf{L10})_3]^{9+}$	34.3	33.9(3)[c,l]
$[Lu(\mathbf{L3})_3]^{3+}$	16.7	17.2(7)[d]	$[Lu_3(\mathbf{L10})_2]^{9+}$	27.1	27.4(5)[c,l]
$[Lu(\mathbf{L4})]^{3+}$	6.2	7.2(2)[c,e]	$[Lu_3(\mathbf{L11})_3]^{9+}$	34.6	35(1)[c,m]
$[Lu(\mathbf{L4})_2]^{3+}$	11.9	11.5(4)[d]	$[Lu_4(\mathbf{L11})_3]^{12+}$	40.1	41(1)[c,m]
$[Lu(\mathbf{L4})_3]^{3+}$	17.2	17.3(4)[d]	$[Lu_4(\mathbf{L11})_2]^{12+}$	31.8	31(1)[c,m]
$[Lu(\mathbf{L5})_3]^{3+}$	17.5	17.1(5)[c,f]	$[Lu_3(\mathbf{L11})_2]^{9+}$	27.2	28(1)[c,m]
$[Lu_2(\mathbf{L5})_3]^{6+}$	25.3	25.4(5)[c,f]			

[a] Calculated by using Equations (12), (16), (18), (20), and S1–S25. [b] Ref. [24]. [c] Spectrophotometric titration, MeCN, 298 K. [d] We have repeated the titration under conditions used for **L1** and **L2** and observe a similar value for $[Lu(\mathbf{L3})_3]^{3+}$ to that determined by potentiometry in reference [26] ($\log\beta_{1,0,3}^{Lu,Zn,L3}=18.1(8)$; MeCN, 298 K). [e] Ref. [27]. [f] Ref. [28]. [g] Ref. [29]; value for Eu^{3+} complex used. [h] Ref. [30]; value for Eu^{3+} complex used. [i] Ref. [31]; value for Eu^{3+} complex used. [j] Ref. [22]. [k] Ref. [32]; value for La^{3+} complex used. [l] Ref. [33]. [m] Ref. [21].

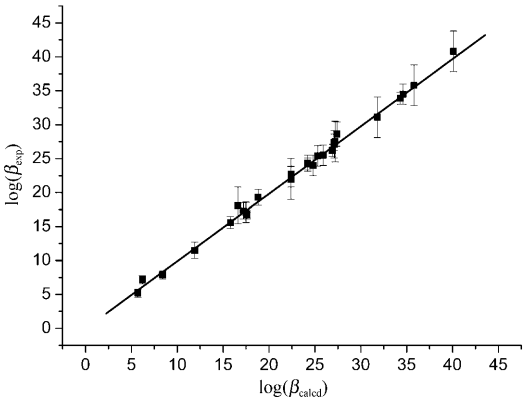

Figure 3. Correlation between experimental and calculated $\log\beta_{m_1,m_2,n}^{Lu,Zn,L\phi}$ ($\phi=1$–11) values (error bars on experimetal values correspond to 3σ).

The global value of $\Delta g_{corr}^{M,L\phi}=23(2)$ kJ mol^{-1} is, however, significantly greater than previous estimates of $\Delta g_{corr}^{M,L\phi}=5(1)$ kJ mol^{-1}.[21] According to the present results, the microscopic affinity of for example the Lu^{3+} ion for the tridentate N_2O and N_3 sites decreases from $\Delta g_{inter}^{Lu,L\phi}=-31(2)$ to $\Delta g_{intra}^{Lu,L\phi}=\Delta g_{inter}^{Lu,L\phi}+\Delta g_{corr}^{M,L\phi}=-8(2)$ kJ mol^{-1} on replacing the intermolecular connection with its intramolecular counterpart, indicating an aversion for (macro)cyclisation comparable to that observed for the covalent lanthanide receptor recently reported by Canard et al. ($\Delta g_{intra}^{Lu,L\phi}=-8.5(4)$ kJ mol^{-1}).[36] This effect can be illustrated qualitatively by simple ESI-MS titrations. Addition of three equivalents of the tridentate ligand **L4** to a solution containing $[Lu_2(\mathbf{L5})_3]^{6+}$ (MeCN, $|\mathbf{L4}|_{tot}=1.5\times10^{-3}$ M; **L5** contains two **L4** units connected by a methylene spacer) indeed leads to the quantitative destruction of the binuclear helicate to give peaks corresponding to mononuclear homoleptic $[Lu(\mathbf{L}\phi)_n]^{3+}$ ($\phi=4$, 5; $n=1$–3) and heteroleptic $[Lu(\mathbf{L4})_n(\mathbf{L5})_{3-n}]^{3+}$ ($n=1$, 2) complexes, in which only intermolecular connections operate. This exposes a severe lack of structural preorganisation in the intermediate species leading to the final polynuclear assemblies. The effective concentrations $c^{eff}\approx10^{-4}$ M for the present system and $c^{eff}\approx10^{-7}$ M for the aforementioned covalent receptor,[36] are

both orders of magnitude lower than the value of $c^{\mathrm{eff}} \approx 10^{-2}$ M predicted for the interaction between two sites separated by 18 Å[37] and connected by an ideal freely jointed chain (excluded volume effects are neglected).[11f] Clearly, the organic linkers which connect adjacent binding sites in the segmental ligands considered herein are far from meeting this criteria. Such a large energy cost of $\Delta g_{\mathrm{corr}}^{\mathrm{M,L}\phi} = 23(2)\ \mathrm{kJ\,mol^{-1}}$ is thus likely a result of unfavourable enthalpic factors, the most pertinent of which are the conformational ring strains exerted upon both the ligand scaffold and the metal–ligand bonds when a pendant binding site is fixed to an unsaturated metal ion during an intramolecular binding event (i.e. $\Delta H_{\mathrm{inter}}^{\mathrm{M,L}\phi} \neq \Delta H_{\mathrm{intra}}^{\mathrm{M,L}\phi}$ and thus the common approximation $c^{\mathrm{eff}} = e^{\left(\Delta S_{\mathrm{intra}}^{\mathrm{M,L}\phi} - \Delta S_{\mathrm{inter}}^{\mathrm{M,L}\phi}\right)/R}$ is no longer valid).

Quantifying cooperativity and preorganisation: According to the Ising and site binding models [Eq. (5)],[17,18] any deviations from statistical binding in a $[\mathrm{Lu}_{m_1}\mathrm{Zn}_{m_2}(\mathbf{L}\phi)_n]^{(3m_1+2m_2)+}$ complex can be assigned to homo-component interactions, which are defined as $\Delta E^{\mathrm{L,L}}$ (interligand) and $\Delta E_{1-x}^{\mathrm{Lu,Lu}}$ and $\Delta E_{1-x}^{\mathrm{Zn,Lu}}$ (intermetallic, with $x=2$ for geminal, $x=3$ for vicinal and $x=4$ for distal) in the present context. The fitted average value of $\Delta E^{\mathrm{L,L}} = 1(2)\ \mathrm{kJ\,mol^{-1}}$ indicates that no severe stereoelectronic effects accompany the coordination of several binding units to the same metal. It can be compared with the mildly repulsive aromatic stacking interactions observed between overlapping phenyl rings in, for example, the hydrogen-bonded zipper complexes reported by Cockroft et al.[38] The five solution-phase intermetallic interactions $\Delta E_{1-x}^{\mathrm{Lu,Lu}}$ and $\Delta E_{1-x}^{\mathrm{Zn,Lu}}$ acting between charged cations separated by about 9 Å ($x=2$), 18 Å ($x=3$) and 27 Å ($x=4$) in the bi-, tri- and tetranuclear complexes of segmental ligands **L1** and **L5**–**11** constitute the most striking features of this investigation. Not only do they deviate by several orders of magnitude from the analogous gas-phase values predicted using the simple Coulomb equation 7, the adjusted $\Delta E_{1-x}^{\mathrm{M,M}}$ parameters in solution even defy any trends anticipated by sole consideration of the latter model (Table 1, the metals are considered as non-polarizable point charges, a rough assumption but compatible with our level of approximation because charge delocalization is limited for 4f block ions and for closed-shell Zn^{2+} with N-donor ligands).[39] Firstly, the geminal interaction $\Delta E_{1-2}^{\mathrm{M,M}}$ between two metals located about 9 Å apart in adjacent binding sites *increases* on decreasing the charge of one of the metals ($\Delta E_{1-2}^{\mathrm{Lu,Lu}} = 4(1)\ \mathrm{kJ\,mol^{-1}} \ll \Delta E_{1-2}^{\mathrm{Zn,Lu}} = 18(2)\ \mathrm{kJ\,mol^{-1}}$). Secondly, the distal $\Delta E_{1-4}^{\mathrm{Lu,Lu}}$ interaction between two Lu^{3+} cations separated by ca. 27 Å is more repulsive than the short-range geminal $\Delta E_{1-2}^{\mathrm{Lu,Lu}}$ interaction ($\Delta E_{1-4}^{\mathrm{Lu,Lu}} = 18(4)\ \mathrm{kJ\,mol^{-1}} \gg \Delta E_{1-2}^{\mathrm{Ln,Lu}} = 4(1)\ \mathrm{kJ\,mol^{-1}}$). And finally, the vicinal interactions $\Delta E_{1-3}^{\mathrm{Lu,Lu}}$ and $\Delta E_{1-3}^{\mathrm{Zn,Lu}}$ acting between both $Lu^{3+}\cdots Lu^{3+}$ and $Zn^{2+}\cdots Lu^{3+}$ pairs separated by about 18 Å appear to be attractive ($\Delta E_{1-3}^{\mathrm{Lu,Lu}} = -8(3)\ \mathrm{kJ\,mol^{-1}}$ and $\Delta E_{1-3}^{\mathrm{Zn,Lu}} = -4(2)\ \mathrm{kJ\,mol^{-1}}$), and thus constitute a source of stabilisation for the tri- and tetranuclear helicates. Indeed, these interactions have a significant impact on the overall stabilities of all the polynuclear complexes considered in the present study, as illustrated by the global cooperativity indices[9c,d] listed in Table 3 (column 3). The cooperativity index I_c^{tot} is simply the product of the various microscopic homo-component interactions ($u^{\mathrm{L,L}}$, $u_{1-x}^{\mathrm{M,M}}$) acting in a given complex [Eq. (21)], and it allows global deviations from statistical binding to be quantified.

$$I_c^{\mathrm{tot}} = I_c^{\mathrm{L,L}} I_c^{\mathrm{M,M}} = \prod_{p<q}''\left(u_{pq}^{\mathrm{L,L}}\right) \prod_{i<j}'''\left(u_{ij}^{\mathrm{M,M}}\right) \tag{21}$$

The cooperativity indices I_c^{tot} computed for the mononuclear complexes $[\mathrm{M}(\mathbf{L}\phi)_n]^{z+}$ ($\phi = 1$–5; $\mathrm{M} = Zn^{2+}$, Lu^{3+}, $n=2$, 3, Table 3) are sufficiently close to zero to suggest statistical binding. The associated energy contributions of $\Delta E_c^{\mathrm{tot}} = -RT\ln\left(I_c^{\mathrm{tot}}\right) \leq 2\ \mathrm{kJ\,mol^{-1}}$ originate from the mildly repulsive interligand interaction $\Delta E^{\mathrm{L,L}} = 1(2)\ \mathrm{kJ\,mol^{-1}}$, but they hold little significance within the margin of experimental error. In contrast, I_c^{tot} values computed for the polynuclear complexes $[\mathrm{Lu}_{m_1}\mathrm{Zn}_{m_2}(\mathbf{L}\phi)_n]^{(3m_1+2m_2)+}$ ($\phi = 1$–11; $m_1 = 0$–4; $m_2 = 0$–1; $n = 2$, 3, Table 3), which include intermetallic interactions, clearly invoke negative cooperativity as a prevailing feature in the present assemblies, in accord with earlier investigations.[9c,d]

Focusing now on preorganisation effects, it is clear that the adjusted value of $\log(c^{\mathrm{eff}}) \approx -4.0(4)$ reflects both entropic (statistical) and enthalpic (ring strain) contributions, that is $c^{\mathrm{eff}} = c_{\mathrm{strain}}^{\mathrm{eff}} c_{\mathrm{stat}}^{\mathrm{eff}} = e^{-\left(\Delta H_{\mathrm{intra}}^{\mathrm{M,L}\phi} - \Delta H_{\mathrm{inter}}^{\mathrm{M,L}\phi}\right)/RT} e^{\left(\Delta S_{\mathrm{intra}}^{\mathrm{M,L}\phi} - \Delta S_{\mathrm{inter}}^{\mathrm{M,L}\phi}\right)/R}$ (vide supra). If the former enthalpic component is expressed as $c_{\mathrm{strain}}^{\mathrm{eff}} \approx c^{\mathrm{eff}}/c_{\mathrm{stat}}^{\mathrm{eff}}$, it indeed corresponds to an additional index $I_{\mathrm{p}}^{\mathrm{strain}} = \prod_{p<q}''''\left(c^{\mathrm{eff}}/c_{\mathrm{stat}}^{\mathrm{eff}}\right)$ measuring the degree of structural preorganisation for intramolecular (macro)cyclisation. Its combination with the cooperativity index in Equation (21) then gives an expression for the total deviation from statistical binding [Eq. (22)] for complexes in which intramolecular interactions occur.

$$I_{c+p}^{\mathrm{tot}} = I_c^{\mathrm{L,L}} I_c^{\mathrm{M,M}} I_p^{\mathrm{strain}} = \prod_{p<q}''\left(u_{pq}^{\mathrm{L,L}}\right) \prod_{i<j}'''\left(u_{ij}^{\mathrm{M,M}}\right) \prod_{i}''''\left(c^{\mathrm{eff}}/c_{\mathrm{stat}}^{\mathrm{eff}}\right) \tag{22}$$

Taking Gargano's values[11(f)] for the effective concentration at optimal polymer length between two interacting sites separated by 18 Å ($c_{1-2,\mathrm{stat}}^{\mathrm{eff}} \approx 10^{-2}$ M)[37] and by 36 Å ($c_{1-3,\mathrm{stat}}^{\mathrm{eff}} \approx 10^{-3}$ M) as rough estimates for the pure statistical contributions, we can then compute preorganisation indices I_p^{strain} (Table 3, column 5) and the total indices for deviations from statistics $I_{c+p}^{\mathrm{strain}}$ (Table 3, column 7). From these values, it is clear that the negative cooperativity operating in the present polynuclear systems is further aggravated by unfavourable preorganisation, eventually causing global deviations from statistics in excess of $\Delta E_{c+p}^{\mathrm{tot}} \approx 20$–$100\ \mathrm{kJ\,mol^{-1}}$ depending on the number of interacting components.

Model and interpretation of the intermetallic interactions: The alarmingly low cation–cation repulsions of $\Delta E_{1-2}^{\mathrm{Eu,Eu}} = 8(4)$–$14(5)\ \mathrm{kJ\,mol^{-1}}$ reported in previous studies[21] have already provoked efforts towards understanding the role of

Table 3. Cooperativity (I_c) and preorganisation (I_p) indices for the formation of complexes $[Lu_{m_1}Zn_{m_2}(\mathbf{L}\phi)_3]^{(3m_1+2m_2)+}$ (ϕ=1–11; m_1=0–4; m_2=0-1; n=2, 3).

Microspecies	$\log(I_c^{L,L})$ ($\Delta E_c^{L,L}$)[b]	$\log(I_c^{M,M})$ ($\Delta E_c^{M,M}$)[b]	$\log(I_c^{tot})$[a] (ΔE_c^{tot})[b]	Cooperativity	$\log(I_p^{strain})$ (ΔE_p^{strain})[b]	Preorganisation	$\log(I_{c+p}^{tot})$[c] (ΔE_{c+p}^{tot})[b]	Total deviation
$[Lu(\mathbf{L1})_3]^{3+}$	−0.4 (2)	–	−0.4 (2)	≈none	–	–	−0.4 (2)	≈none
$[Lu_2(\mathbf{L1})_3]^{6+}$	−0.9 (5)	−0.6 (4)	−1.5 (9)	negative	−4.3 (25)	negative	−5.8 (33)	negative
$[Lu_2Zn(\mathbf{L1})_3]^{8+}$	−1.3 (7)	−3.0 (17)	−4.3 (24)	negative	−8.6 (49)	negative	−12.9 (73)	negative
$[Zn(\mathbf{L1})_3]^{2+}$	-0.4 (2)	–	−0.4 (2)	≈none	–	–	−0.4 (2)	≈none
$[Zn(\mathbf{L2})]^{2+}$	-	–	–	–	–	–	–	–
$[Zn(\mathbf{L2})_2]^{2+}$	−0.1 (1)	–	−0.1 (1)	≈ none	–	–	−0.1 (1)	≈ none
$[Zn(\mathbf{L2})_3]^{2+}$	−0.4 (2)	–	−0.4 (2)	≈none	–	–	−0.4 (2)	≈none
$[Lu(\mathbf{L3})_3]^{3+}$	−0.4 (2)	–	−0.4 (2)	≈none	–	–	−0.4 (2)	≈none
$[Lu(\mathbf{L4})]^{3+}$	-	–	–	–	–	–	–	–
$[Lu(\mathbf{L4})_2]^{3+}$	−0.1 (1)	–	−0.1 (1)	≈none	–	–	−0.1 (1)	≈none
$[Lu(\mathbf{L4})_3]^{3+}$	−0.4 (2)	–	−0.4 (2)	≈none	–	–	−0.4 (2)	≈none
$[Lu(\mathbf{L5})_3]^{3+}$	−0.4 (2)	–	−0.4 (2)	≈none	–	–	−0.4 (2)	≈none
$[Lu_2(\mathbf{L5})_3]^{6+}$	-0.9 (5)	−0.6 (4)	−1.5 (9)	negative	−4.3 (25)	negative	−5.8 (33)	negative
$[Lu_2(\mathbf{L5})_2]^{6+}$	−0.3 (2)	−0.6 (4)	−0.9 (6)	negative	−2.1 (12)	negative	−3.1 (18)	negative
$[Lu_2(\mathbf{L6})_3]^{6+}$	−0.9 (5)	−0.6 (4)	−1.5 (9)	negative	−4.3 (25)	negative	−5.8 (33)	negative
$[Lu_2(\mathbf{L7})_3]^{6+}$	−0.9 (5)	−0.6 (4)	−1.5 (9)	negative	−4.3 (25)	negative	−5.8 (33)	negative
$[LuZn(\mathbf{L8})_3]^{5+}$	−0.9 (5)	−3.1 (18)	−4.0 (23)	negative	−4.3 (25)	negative	−8.3 (47)	negative
$[LuRu(\mathbf{L8})_3]^{5+}$	−0.4 (2)	−3.1 (18)	−3.6 (20)	negative	−4.3 (25)	negative	−7.9 (45)	negative
$[Zn(\mathbf{L8})_3]^{2+}$	−0.4 (2)	–	−0.4 (2)	≈none	–	–	−0.4 (2)	≈ none
$[LuZn(\mathbf{L9})_3]^{5+}$	−0.9 (5)	−3.1 (18)	−4.0 (23)	negative	−4.3 (25)	negative	−8.3 (47)	negative
$[Lu_2(\mathbf{L10})_3]^{6+}$								
ttt,ttt	−0.9 (5)	1.3 (−8)	0.5 (−3)	positive	−4.3 (25)	negative	−3.8 (22)	negative
ttt,ccc	−0.9 (5)	−0.6 (4)	−1.5 (9)	negative	−4.3 (25)	negative	−5.8 (33)	negative
ctt,tcc	−0.9 (5)	−0.6 (4)	−1.5 (9)	negative	−4.3 (25)	negative	−5.8 (33)	negative
$[Lu_3(\mathbf{L10})_3]^{9+}$	−1.3 (7)	0.1 (−1)	−1.2 (6)	negative	−8.6 (49)	negative	−9.8 (56)	negative
$[Lu_3(\mathbf{L10})_2]^{9+}$	-0.4 (2)	0.1 (−1)	−0.3 (2)	negative	−4.3 (25)	negative	−4.6 (26)	negative
$[Lu_3(\mathbf{L11})_3]^{9+}$								
ttt,ccc,ttt	−1.3 (7)	−2.4 (14)	−3.7 (21)	negative	−8.6 (49)	negative	−12.3 (70)	negative
ttt,ccc,ccc	−1.3 (7)	0.1 (−1)	−1.2 (6)	negative	−8.6 (49)	negative	−9.8 (56)	negative
ttc,ccc,cct	−1.3 (7)	0.1 (−1)	−1.2 (6)	negative	−8.6 (49)	negative	−9.8 (56)	negative
$[Lu_4(\mathbf{L11})_3]^{12+}$	−1.7 (10)	−2.3 (13)	−4.1 (23)	negative	−12.9 (74)	negative	−17.0 (97)	negative
$[Lu_4(\mathbf{L11})_2]^{12+}$	−0.6 (3)	−2.3 (13)	-2.9 (17)	negative	−6.4 (37)	negative	−9.4 (53)	negative
$[Lu_3(\mathbf{L11})_2]^{9+}$								
tt,cc,tt	−0.4 (2)	−2.4 (14)	−2.9 (16)	negative	−4.3 (25)	negative	−7.2 (41)	negative
tt,cc,cc	−0.4 (2)	0.1 (−1)	−0.3 (2)	negative	−4.3 (25)	negative	−4.6 (26)	negative
ct,cc,tc	−0.4 (2)	0.1 (−1)	−0.3 (2)	negative	−4.3 (25)	negative	−4.6 (26)	negative

[a] Calculated by using Equation (21),[9c,d] from the fitted parameters listed in Table 1. [b] Values in kJ mol^{-1} are given in parentheses. [c] Calculated by using Equation (22).

charge interaction in self-assembly processes. To date, they have been modeled semi-quantitatively in terms of the solvation changes which accompany the accumulation of charge when one-dimensional multi-component assemblies undergo a sequential increase in nuclearity.[22] Owing to insufficient data redundancy, however, the previous estimates of $\Delta E_{1-2}^{Eu,Eu}$ were obtained from fits in which intermetallic interactions were constrained to obey the Coulomb law [Eq. (7)], an approach which is now considered inappropriate. Moreover, such limitations prevented access to information concerning the evolution of the intermetallic interactions as a function of separation along a polynuclear array. The complete set of $\Delta E_{1-x}^{M,M}$ values obtained from the current study not only enable us to address this latter point, they further present an opportunity to globally model the apparent interactions occurring in solution between pairs of differently charged cations (3+,3+ *and* 2+,3+) separated by any one of the three intermetallic distances, 9, 18 or 27 Å characteristic of the present linear polymetallic helicates. In attempt to first understand the somewhat counter-intuitive relationship between the solution-phase intermetallic interactions $\Delta E_{1-x}^{M,M}$ (x=1-4) and charge separation (d), the following section will consider selected microspecies in the self-assembly pathways leading to the trinuclear helicate $[Lu_3(\mathbf{L10})_3]^{9+}$ (for M=Lu^{3+} and x=2, 3) and the tetranuclear helicate $[Lu_4(\mathbf{L11})_3]^{12+}$ (for M=Lu^{3+} and x=4). The effects of cation charge will then be similarly assessed by further taking into consideration the bimetallic helicate *HHH*-$[Lu_2Zn(\mathbf{L1})_3]^{8+}$, in which the presence of both a Zn^{2+} dication and two Lu^{3+} trications gives rise to the two additional interaction terms $\Delta E_{1-2}^{Zn,Lu}$ and $\Delta E_{1-3}^{Zn,Lu}$.

Dependence of $\Delta E_{1-x}^{M,M}$ on charge separation *d*: For those who are not familiar with extended modelling of metal–ligand assembly processes, they can skip the forthcoming derivation and directly consider the final Equations (47)–(49). However, our approach to modelling intermetallic interactions in solution combines appropriate Born–Haber cycles with the Born Equation (7), and it is a crucial aspect of this contribution. As a demonstration, therefore, we will

derive expressions for the geminal (1-2) and vicinal (1-3) interactions acting between two Lu^{3+} trications in the following section, whilst derivations for the remaining $\Delta E_{1-x}^{M,M}$ terms can be found in the Supporting Information. Let us now consider the formation of the three selected microspecies *t*-$[Lu(\mathbf{L10})_3]^{3+}$, *tc*-$[Lu_2(\mathbf{L10})_3]^{6+}$ and $[Lu_3(\mathbf{L10})_3]^{9+}$ (equilibria (23)–(25), Figure 4), for which the corresponding microscopic stability constants $\beta_{m_1,0,3}^{Lu,Zn,\mathbf{L10}}$ ($m_1=1$–3) are expressed in Equations (26)–(28), respectively (the statistical factors are given in Table S1 in the Supporting Information).[40]

$$3\,\mathbf{L10} + Lu^{3+} \rightleftharpoons t\text{-}[Lu(\mathbf{L10})_3]^{3+} \quad \beta_{1,0,3}^{Lu,Zn,\mathbf{L10}} \tag{23}$$

$$3\,\mathbf{L10} + 2\,Lu^{3+} \rightleftharpoons tc\text{-}[Lu_2(\mathbf{L10})_3]^{6+} \quad \beta_{2,0,3}^{Lu,Zn,\mathbf{L10}} \tag{24}$$

$$3\,\mathbf{L10} + 3\,Lu^{3+} \rightleftharpoons [Lu_3(\mathbf{L10})_3]^{9+} \quad \beta_{3,0,3}^{Lu,Zn,\mathbf{L10}} \tag{25}$$

$$\beta_{1,0,3}^{Lu,Zn,\mathbf{L10}} = 32\left(f_{N_2O}^{Lu}\right)^3\left(u^{L,L}\right)^3 \tag{26}$$

$$\beta_{2,0,3}^{Lu,Zn,\mathbf{L10}} = 192\left(f_{N_2O}^{Lu}\right)^3\left(f_{N_3}^{Lu}\right)^3\left(u^{L,L}\right)^6\left(c^{eff}\right)^2\left(u_{1-2}^{Lu,Lu}\right) \tag{27}$$

$$\beta_{3,0,3}^{Lu,Zn,\mathbf{L10}} = 576\left(f_{N_2O}^{Lu}\right)^6\left(f_{N_3}^{Lu}\right)^3\left(u^{L,L}\right)^9\left(c^{eff}\right)^4\left(u_{1-2}^{Lu,Lu}\right)^2\left(u_{1-3}^{Lu,Lu}\right) \tag{28}$$

The associated successive stability constants K_1–K_3 [Eq. (23), (29) and (30)] corresponding to the fixation of i) a first Lu^{3+} ion to three co-aligned strands of **L10** ($K_1=\beta_{1,0,3}^{Lu,Zn,\mathbf{L10}}$), ii) a second Lu^{3+} ion to the now pre-assembled *t*-$[Lu(\mathbf{L10})_3]^{3+}$ receptor (K_2) and iii) a third Lu^{3+} ion to the now pre-assembled *tc*-$[Lu_2(\mathbf{L10})_3]^{6+}$ receptor (K_3), are given by Equations (31)–(33) (see Figure 4 for schematic structures of the complexes).

$$t\text{-}[Lu(\mathbf{L10})_3]^{3+} + Lu^{3+} \rightleftharpoons tc\text{-}[Lu_2(\mathbf{L10})_3]^{6+} \tag{29}$$

$$tc\text{-}[Lu_2(\mathbf{L10})_3]^{6+} + Lu^{3+} \rightleftharpoons [Lu_3(\mathbf{L10})_3]^{9+} \tag{30}$$

$$K_1 = \beta_{1,0,3}^{Lu,Zn,\mathbf{L10}} = 32\left(f_{N_2O}^{Lu}\right)^3\left(u^{L,L}\right)^3 \tag{31}$$

$$K_2 = \frac{\beta_{2,0,3}^{Lu,Zn,\mathbf{L10}}}{\beta_{1,0,3}^{Lu,Zn,\mathbf{L10}}} = \frac{192\left(f_{N_2O}^{Lu}\right)^3\left(f_{N_3}^{Lu}\right)^3\left(u^{L,L}\right)^6\left(c^{eff}\right)^2\left(u_{1-2}^{Lu,Lu}\right)}{32\left(f_{N_2O}^{Lu}\right)^3\left(u^{L,L}\right)} = 6\left(f_{N_3}^{Lu}\right)^3\left(u^{L,L}\right)^3\left(c^{eff}\right)^2\left(u_{1-2}^{Lu,Lu}\right) \tag{32}$$

$$K_3 = \frac{\beta_{3,0,3}^{Lu,Zn,\mathbf{L10}}}{\beta_{2,0,3}^{Lu,Zn,\mathbf{L10}}} = \frac{576\left(f_{N_2O}^{Lu}\right)^6\left(f_{N_3}^{Lu}\right)^3\left(u^{L,L}\right)^9\left(c^{eff}\right)^4\left(u_{1-2}^{Lu,Lu}\right)^2\left(u_{1-3}^{Lu,Lu}\right)}{192\left(f_{N_2O}^{Lu}\right)^3\left(f_{N_3}^{Lu}\right)^3\left(u^{L,L}\right)^6\left(c^{eff}\right)^2\left(u_{1-2}^{Lu,Lu}\right)} = 3\left(f_{N_2O}^{Lu}\right)^3\left(u^{L,L}\right)^3\left(c^{eff}\right)^2\left(u_{1-2}^{Lu,Lu}\right)\left(u_{1-3}^{Lu,Lu}\right) \tag{33}$$

Since the microscopic affinities of Lu^{3+} for the tridentate N_3 and N_2O sites are similar, that is $f_{N_2O}^{Lu} \approx f_{N_3}^{Lu}$, the difference in Gibbs free energy between the assembly of a tripodal receptor *t*-$[Lu(\mathbf{L10})_3]^{3+}$ and the successive complexation of a second, geminal Lu^{3+} ion, can be reasonably expressed as Equation (34). The same treatment employing K_2 [Eq. (32)] and K_3 [Eq. (33)] provides an equivalent expression for the free energy difference between successive complexations of the second (geminal) and third (vicinal) Lu^{3+} ions to *t*-$[Lu(\mathbf{L10})_3]^{3+}$ [Eq. (35)].

$$\Delta G_{K_2}^0 - \Delta G_{K_1}^0 = -RT\ln\left(\frac{K_2}{K_1}\right) = -RT\ln\left(\frac{6\left(f_{N_3}^{Lu}\right)^3\left(u^{L,L}\right)^3\left(c^{eff}\right)^2\left(u_{1-2}^{Lu,Lu}\right)}{32\left(f_{N_2O}^{Lu}\right)^3\left(u^{L,L}\right)^3}\right) = -RT\ln\left(\frac{3}{16}\left(c^{eff}\right)^2\left(u_{1-2}^{Lu,Lu}\right)\right) \tag{34}$$

$$\Delta G_{K_3}^0 - \Delta G_{K_2}^0 = -RT\ln\left(\frac{K_3}{K_2}\right) = -RT\ln\left(\frac{3\left(f_{N_2O}^{Lu}\right)^3\left(u^{L,L}\right)^3\left(c^{eff}\right)^2\left(u_{1-2}^{Lu,Lu}\right)\left(u_{1-3}^{Lu,Lu}\right)}{6\left(f_{N_3}^{Lu}\right)^3\left(u^{L,L}\right)^3\left(c^{eff}\right)^2\left(u_{1-2}^{Lu,Lu}\right)}\right) = -RT\ln\left(\frac{\left(u_{1-3}^{Lu,Lu}\right)}{2}\right) \tag{35}$$

Substituting Boltzmann terms for the intermetallic interactions $u_{1-x}^{Lu,Lu} = e^{-\Delta E_{1-x}^{Lu,Lu}/RT}$ into Equations (34) and (35), followed by rearrangement, then gives Equations (36) and (37), which show that the free energy differences $\Delta G_{K_n}^0 - \Delta G_{K_{n-1}}^0$ depend principally on i) a geminal (1-2) or a vicinal (1-3) intermetallic interaction $\Delta E_{1-x}^{Lu,Lu}$ ($x=2$, 3), ii) the ratio of the statistical factors for the two equilibria concerned, and iii) in the case of $\Delta G_{K_2}^0 - \Delta G_{K_1}^0$, the effective concentration c^{eff}.

$$\Delta G_{K_2}^0 - \Delta G_{K_1}^0 = \Delta E_{1-2}^{Lu,Lu} + RT\ln\left(\frac{16}{3}\right) - 2RT\ln\left(c^{eff}\right) \tag{36}$$

$$\Delta G_{K_3}^0 - \Delta G_{K_2}^0 = \Delta E_{1-3}^{Lu,Lu} + RT\ln(2) \tag{37}$$

Assuming that the standard $\Delta E_{1-x,gas}^{Lu,Lu} \propto {}^1/_d$ dependency prevails in the gas-phase according to the Coulomb law [Eq. (7), $\varepsilon_r=1$], substituting $\Delta E_{1-x}^{Lu,Lu}$ in Equations (36) and (37) by appropriate Coulomb terms gives Equations (38) and (39), which describe the analogous free energy differences operating exclusively in the gas-phase.

$$\Delta G_{K_2,gas}^0 - \Delta G_{K_1,gas}^0 = \frac{\left(z_{Lu}\right)^2 e^2 N_A}{4\pi\varepsilon_0 d} + RT\ln\left(\frac{16}{3}\right) - 2RT\ln\left(c_{gas}^{eff}\right) \tag{38}$$

$$\Delta G_{K_3,gas}^0 - \Delta G_{K_2,gas}^0 = \frac{\left(z_{Lu}\right)^2 e^2 N_A}{4\pi\varepsilon_0 2d} + RT\ln(2) \tag{39}$$

Several points are worth noting here. Firstly, the regular geminal separations of $d \approx 9$ Å, systematically observed in all related polynuclear triple-stranded helicates reported to date, allow for the assumption that two metals separated by two binding sites (i.e. the 1-3 vicinal interaction as required in the Coulomb term for $\Delta E^{Lu,Lu}_{1-3,gas}$) lie ca. $2d \approx 18$ Å apart. Secondly, although the gas-phase statistical factors $\omega_{K_n,gas}$ for Equilibria (23), (29) and (30) are not necessarily the same as their solution-phase counterparts (see Table S1 in the Supporting Information), the ratio $\omega_{K_n,gas}/\omega_{K_{n-1},gas}$ equate to $\omega_{K_n,sol}/\omega_{K_{n-1},sol}$ and consequently no further modifications are required when expressing the Gibbs free energy differences $(\Delta G^0_{K_n} - \Delta G^0_{K_{n-1}})$ in the gas-phase.

According to the Born–Haber cycles depicted in Figure 4, the quantities $\Delta G^0_{K_n,gas} - \Delta G^0_{K_{n-1},gas}$ formulated in Equations (38) ($n=2$) and (39) ($n=3$) can be alternatively approached as simple additive contributions of i) the solution-phase free energy differences $\Delta G^0_{K_n} - \Delta G^0_{K_{n-1}}$ [previously defined in Equations (34) and (35)] and ii) the solvation energies $\Delta_{solv}G^0$ of the participating species. This leads to Equations (40) and (41), where the solvation energies of complex cations *t*-$[Lu(\mathbf{L10})_3]^{3+}$ ($\Delta_{solv}G^0_{Lu(\mathbf{L10})_3}$), *tc*-$[Lu_2(\mathbf{L10})_3]^{6+}$ ($\Delta_{solv}G^0_{Lu_2(\mathbf{L10})_3}$) and $[Lu_3(\mathbf{L10})_3]^{9+}$ ($\Delta_{solv}G^0_{Lu_3(\mathbf{L10})_3}$) may be estimated using the Born equation [Eq. (8)], provided that the pseudo-spherical or *effective* radius ($r = R_0^{Lu_x(\mathbf{L10})_3}$, where $x =$ 1–3) of each species is accessible.

$$\Delta G^0_{K_2,gas} - \Delta G^0_{K_1,gas} = \Delta G^0_{K_2,sol} - \Delta G^0_{K_1,sol} + 2\Delta_{solv}G^0_{Lu(\mathbf{L10})_3} - \Delta_{solv}G^0_{Lu_2(\mathbf{L10})_3} - 3\Delta_{solv}G^0_{\mathbf{L10}} \quad (40)$$

$$\Delta G^0_{K_3,gas} - \Delta G^0_{K_2,gas} = \Delta G^0_{K_3,sol} - \Delta G^0_{K_2,sol} + 2\Delta_{solv}G^0_{Lu_2(\mathbf{L10})_3} - \Delta_{solv}G^0_{Lu_3(\mathbf{L10})_3} - \Delta_{solv}G^0_{Lu(\mathbf{L10})_3} \quad (41)$$

Since metals are sequentially added in one dimension along the helical axis in going from *t*-$[Lu(\mathbf{L10})_3]^{3+}$ to *tc*-$[Lu_2(\mathbf{L10})_3]^{6+}$ and finally $[Lu_3(\mathbf{L10})_3]^{9+}$, we reasonably assume that the resulting stepwise rigidification produces a linear increase of the effective radius. $R^{Lu_x(\mathbf{L10})_3}$ ($x=2$, 3) are thus given by $R^{Lu_x(\mathbf{L10})_3} = R_0^{Lu(\mathbf{L10})_3}(1 + \alpha d(x-1))$, where $R^{Lu_x(\mathbf{L10})_3}$ is the effective radius of the initial tripodal receptor *t*-$[Lu(\mathbf{L10})_3]^{3+}$, d is the geminal intermetallic separation (ca. 9 Å), x is the total number of metal ions in the complex and α is an expansion coefficient. The product αd is set to amount to an expansion of 0–15%, as previously observed by diffusion ordered spectroscopy (DOSY) on complexation of Lu^{3+} to the tripodal receptor *HHH*-$[Ru(\mathbf{L8})_3]^{2+}$.[22] With this in mind, the solvation energies of *t*-$[Lu(\mathbf{L10})_3]^{3+}$, *tc*-$[Lu_2(\mathbf{L10})_3]^{6+}$ and $[Lu_3(\mathbf{L10})_3]^{9+}$ take the form given in Equations (42)–(44):

$$\Delta_{solv}G^0_{Lu(\mathbf{L10})_3} = -\frac{(z_{Lu})^2 e^2 N_A}{8\pi\varepsilon_0 R_0^{Lu(\mathbf{L10})_3}}\left(1 - \frac{1}{\varepsilon_r}\right) \quad (42)$$

$$\Delta_{solv}G^0_{Lu_2(\mathbf{L10})_3} = -\frac{(2z_{Lu})^2 e^2 N_A}{8\pi\varepsilon_0 R_0^{Lu(\mathbf{L10})_3}(1+\alpha d)}\left(1 - \frac{1}{\varepsilon_r}\right) \quad (43)$$

$$\Delta_{solv}G^0_{Lu_3(\mathbf{L10})_3} = -\frac{(3z_{Lu})^2 e^2 N_A}{8\pi\varepsilon_0 R_0^{Lu(\mathbf{L10})_3}(1+2\alpha d)}\left(1 - \frac{1}{\varepsilon_r}\right) \quad (44)$$

Inserting the relevant terms for $\Delta G^0_{K_n,sol} - \Delta G^0_{K_{n-1},sol}$ [Eqs. (36), (37)], $\Delta G^0_{K_n,gas} - \Delta G^0_{K_{n-1},gas}$ [Eqs. (38), (39)] and $\Delta_{solv}G^0$ [Eqs. (42)–(44)] into Equations (40) and (41), followed by rearrangement, then gives:

$$\Delta G^0_{K_2,gas} - \Delta G^0_{K_1,gas} = \frac{(z_{Lu})^2 e^2 N_A}{4\pi\varepsilon_0 d} + RT\ln\left(\frac{16}{3}\right) - 2RT\ln\left(c^{eff}_{gas}\right) = \Delta E^{Lu,Lu}_{1-2} + RT\ln\left(\frac{16}{3}\right) - 2RT\ln\left(c^{eff}_{sol}\right) + \frac{(z_{Lu})^2 e^2 N_A}{4\pi\varepsilon_0 R_0^{Lu(\mathbf{L10})_3}}\left(1 - \frac{1}{\varepsilon_r}\right)\left(\frac{1-\alpha d}{1+\alpha d}\right) - 3\Delta_{solv}G^0_{\mathbf{L10}} \quad (45)$$

and

$$\Delta G^0_{K_3,gas} - \Delta G^0_{K_2,gas} = \frac{(z_{Lu})^2 e^2 N_A}{4\pi\varepsilon_0 2d} + RT\ln(2) = \Delta E^{Lu,Lu}_{1-3} + RT\ln(2) + \frac{(z_{Lu})^2 e^2 N_A}{4\pi\varepsilon_0 R_0^{Lu(\mathbf{L10})_3}}\left(1 - \frac{1}{\varepsilon_r}\right)\left(\frac{(\alpha d-1)^2}{(1+\alpha d)(1+2\alpha d)}\right) \quad (46)$$

From which, the solution-phase intermetallic interaction $\Delta E^{Lu,Lu}_{1-x}$ can be easily estimated in the final formulation as Equations (47) and (48) [the assumption that c^{eff} remains unchanged on passing from solution to the gas-phase, that is $c^{eff}_{gas} \approx c^{eff}_{sol}$ has been made for Eq. (47)]:

$$\Delta E^{Lu,Lu}_{1-2} = \frac{(z_{Lu})^2 e^2 N_A}{4\pi\varepsilon_0}\left(\frac{1}{d} - \frac{1}{R_0^{Lu(\mathbf{L10})_3}}\left(1 - \frac{1}{\varepsilon_r}\right)\left(\frac{(1-\alpha d)}{(1+\alpha d)}\right)\right) + 3\Delta_{solv}G^0_{\mathbf{L10}} \quad (47)$$

$$\Delta E^{Lu,Lu}_{1-3} = \frac{(z_{Lu})^2 e^2 N_A}{4\pi\varepsilon_0}\left(\frac{1}{2d} - \frac{1}{R_0^{Lu(\mathbf{L10})_3}}\left(1 - \frac{1}{\varepsilon_r}\right)\left(\frac{(\alpha d-1)^2}{(1+\alpha d)(1+2\alpha d)}\right)\right) \quad (48)$$

A similar derivation based on selected microspecies leading to the formation of the tetranuclear helicate $[Lu_4(\mathbf{L11})_3]^{12+}$ (see Supporting Information, Appendix 3), allows eventual access to the distal 1–4 interaction term $\Delta E^{Lu,Lu}_{1-4}$ operating between two Lu^{3+} cations separated by about $3d \approx 27$ Å [Eq. (49)], $R_0^{Lu(\mathbf{L11})_3}$ is the effective radius of the initial tripodal receptor *t*-$[Lu(\mathbf{L11})_3]^{3+}$.

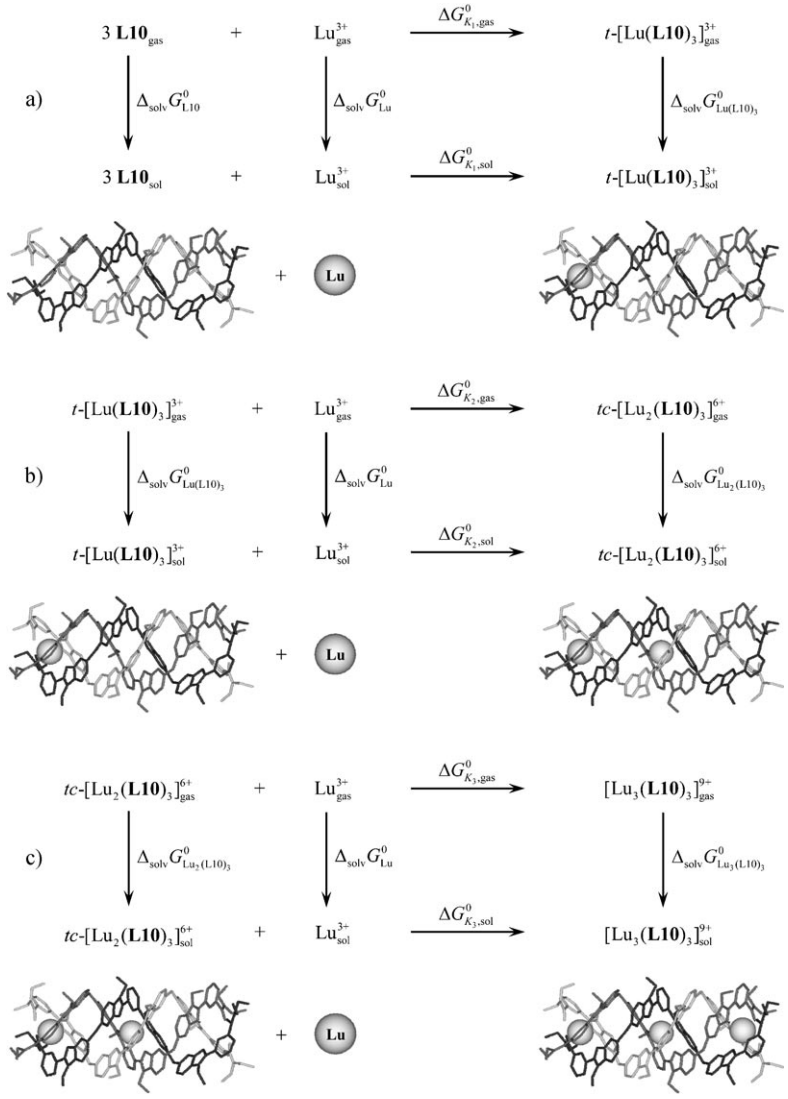

Figure 4. Born–Haber cycles for the successive complexation of Lu^{3+} to a) three strands of **L10**, (b) *t*-$[Lu(\mathbf{L10})_3]^{3+}$ and (c) *tc*-$[Lu_2(\mathbf{L10})_3]^{6+}$ to give $[Lu_3(\mathbf{L10})_3]^{9+}$.

$$\Delta E_{1-4}^{Lu,Lu} = \frac{(z_{Lu})^2 e^2 N_A}{4\pi\varepsilon_0} \left(\frac{1}{3d} - \frac{1}{R_0^{Lu(\mathbf{L11})_3}}\left(1-\frac{1}{\varepsilon_r}\right)\left(\frac{(\alpha d-1)^2}{(1+\alpha d)(1+2\alpha d)(1+3\alpha d)}\right)\right) \quad (49)$$

We are now equipped to model the three apparent solution-phase interactions $\Delta E_{1-x}^{Lu,Lu}$ ($x=2$–4) extracted from the multiple non-linear regression analysis presented in the previous section. We do, however, first require estimates for the effective radii $R_0^{Lu(\mathbf{L10})_3}$ and $R_0^{Lu(\mathbf{L11})_3}$, taken as the pseudo-spherical hydrodynamic radii of the large cations in solution,[23b] and for the expansion coefficient αd in solution. We have thus resorted to measuring auto-diffusion coefficients D_x by DOSY,[41] which transform into pseudo-spherical hydrodynamic radii (r_H^x) using the Stokes–Einstein Equation (50)[42] modified for the size of the diffusing molecules (Table 4, k is Boltzmann's constant, T is the temperature and $\eta = 3.65\times10^{-4}\,kg\,m^{-1}\,s^{-1}$ is the viscosity of acetonitrile at 293 K, $r_{solv}/r_H^x = D_x/D_{solv}$ is the ratio of the experimental diffusion coefficients of the complex and solvent molecules).[43]

$$D_x = \left(\frac{kT}{6\pi\eta r_H^x}\right)\left(1+0.695\left(r_{solv}/r_H^x\right)^{2.234}\right) \quad (50)$$

Starting from the hydrodynamic radii obtained for the mononuclear complexes $[Lu(\mathbf{L4})_3]^{3+}$ ($r_H^{Lu(\mathbf{L4})_3} = 5.84(2)$ Å) and *HHH*-$[Lu(\mathbf{L5})_3]^{3+}$ ($r_H^{Lu(\mathbf{L5})_3} = 7.86(5)$ Å, Table 4), we deduce that the connection of each additional non-coordinated tridentate binding unit increases the effective radius by about 36%. Since **L10** is conceptually obtained from **L5** via the connection of an additional tridentate binding unit, we compute $R_0^{Lu(\mathbf{L10})_3} \approx r_H^{Lu(\mathbf{L5})_3}(1+0.36) =$ 10.7 Å. The same approach applies on going from **L10** to **L11** (i.e. the connection of one additional tridentate binding unit) and $R_0^{Lu(\mathbf{L11})_3} \approx r_H^{Lu(\mathbf{L5})_3}$-$(1+2\times0.36) = 13.4$ Å for *t*-$[Lu(\mathbf{L11})_3]^{3+}$. The incremental expansion (αd) caused by the successive complexation of Lu^{3+}

Table 4. Experimental auto-diffusion coefficients (D_x), calculated hydrodynamic radii [r_H^x, Eq. (50)] and estimated effective radii (R_0^x) for selected $[Lu_{m_1}Zn_{m_2}(\mathbf{L}\phi)_3]^{(3m_1+2m_2)+}$ complexes.

Complex	D_x [$\times10^{-10}$ m^{2}s^{-1}][a]	r_H^x [Å]	R_0^x [Å]
$[Zn(\mathbf{L2})_3]^{2+}$	12.38(1)	5.33(2)	–
$[Lu(\mathbf{L4})_3]^{3+}$	11.12(2)	5.84(2)	–
HHH-$[Lu(\mathbf{L5})_3]^{3+}$	7.92(2)	7.86(5)	–
$[Lu_2(\mathbf{L5})_3]^{6+}$	7.23(3)	8.56(6)	–
HHH-$[Lu_2(\mathbf{L1})_3]^{6+}$	6.26(3)	9.80(6)	–
HHH-$[Zn(\mathbf{L1})_3]^{2+}$	–	–	9.0
HHH-$[Lu_2Zn(\mathbf{L1})_3]^{8+}$	5.86(5)	10.4(1)	–
t-$[Lu(\mathbf{L10})_3]^{3+}$	–	–	10.7
$[Lu_3(\mathbf{L10})_3]^{9+}$	5.5(3)	11.2(6)	–
t-$[Lu(\mathbf{L11})_3]^{3+}$	–	–	13.4
$[Lu_4(\mathbf{L11})_3]^{12+}$	3.9(4)	15.6(7)	–

[a] Measured by DOSY at 293 K, $|\text{complex}|_{tot} = 5\times10^{-3}$ M in CD_3CN.

ions can likewise be placed in the range 5-10% according to the respective increases in hydrodynamic radii observed on going from *HHH*-$[Lu(\mathbf{L5})_3]^{3+}$ ($r_H^{Lu(\mathbf{L5})_3} = 7.86(5)$ Å) to $[Lu_2(\mathbf{L5})_3]^{6+}$ ($r_H^{Lu_2(\mathbf{L5})_3} = 8.56(5)$ Å, 9% increase, Table 4), or from *HHH*-$[Lu_2(\mathbf{L1})_3]^{6+}$ ($r_H^{Lu_2(\mathbf{L1})_3} = 9.80(5)$ Å) to *HHH*-$[Lu_2Zn(\mathbf{L1})_3]^{8+}$ ($r_H^{Lu_2Zn(\mathbf{L1})_3} = 10.4(1)$, 6% increase, Table 4). This leaves only the solvation energy of **L10**, $\Delta_{solv}G^0_{\mathbf{L10}}$, which appears as a dispersive term in Equation (47) for modelling the intermetallic geminal (1-2) interaction. Lacking a straightforward experimental procedure for measuring this quantity, we momentarily focus on modelling only the 1–3 and 1–4 interactions. Inserting values of $R_0^{Lu(\mathbf{L10})_3} \approx r_H^{Lu(\mathbf{L10})_3} = 10.7$ Å for *t*-$[Lu(\mathbf{L10})_3]^{3+}$, $R_0^{Lu(\mathbf{L11})_3} \approx r_H^{Lu(\mathbf{L11})_3} = 13.4$ Å for *t*-$[Lu(\mathbf{L11})_3]^{3+}$ and an upper limit of $\alpha d = 9\%$ into eqs 48 and 49 gives $\Delta E_{1-3}^{Lu,Lu} = -7$ kJ mol^{-1} and $\Delta E_{1-4}^{Lu,Lu} = 66$ kJ mol^{-1}. These values do not only fall within the same orders of magnitudes as their experimental counterparts ($\Delta E_{1-3}^{Lu,Lu} = -8(3)$ kJ mol^{-1} and $\Delta E_{1-4}^{Lu,Lu} = 18(4)$ kJ mol^{-1}, Table 1), they also show the same trends as the latter: $\Delta E_{1-3}^{Lu,Lu} < 0$ and $|\Delta E_{1-4}^{Lu,Lu}| > |\Delta E_{1-3}^{Lu,Lu}|$. By varying the input parameters within the defined ranges of $9.7 \le R_0^{Lu(\mathbf{L10})_3} \approx 10.7 \le 11.7$ Å, $12.4 \le R_0^{Lu(\mathbf{L11})_3} \approx 13.4 \le 14.4$ Å and $5 \le \alpha d \le 10\%$, the experimental values of $\Delta E_{1-3}^{Lu,Lu} = -8(3)$ kJ mol^{-1} and $\Delta E_{1-4}^{Lu,Lu} = 18(4)$ kJ mol^{-1} are then matched perfectly when $R_0^{Lu(\mathbf{L10})_3} = 11.17$ Å, $R_0^{Lu(\mathbf{L11})_3} = 12.97$ Å and $\alpha d = 8.23\%$, values which lie well within the margin of experimental error associated with the initial estimates. Inserting these parameters into Equation (47) further allows the solvation energy of **L10** to be calculated at $\Delta_{solv}G^0_{\mathbf{L10}} \approx -150$ kJ mol^{-1}. Density functional theory (DFT) calculations were performed to estimate the solvation energies of **L10** and **L1** (details are given in the experimental section). It is noteworthy that $\Delta_{solv}G^0_{\mathbf{L10}} \approx -150$ kJ mol^{-1} falls remarkably close to that of $\Delta_{solv}G^0_{\mathbf{L10}} \approx \Delta_{solv}G^0_{\mathbf{L1}} \approx -200$ to -270 kJ mol^{-1} estimated from DFT calculations, despite the simplicity of the purely electrostatic approach used to access the former value. It is also interesting to compare the pseudo-spherical radii of the ion-saturated complexes $[Lu_3(\mathbf{L10})_3]^{9+}$ and $[Lu_4(\mathbf{L11})_3]^{12+}$, extrapolated from $R_0^{Lu(\mathbf{L}\phi)_3}$ by implementing the appropriate size-increases, with those determined experimentally by DOSY for these saturated species. Radii of $R_{calc}^{Lu_3(\mathbf{L10})_3} = R_0^{Lu(\mathbf{L10})_3}(1+2\alpha d) = 13.0$ Å for $[Lu_3(\mathbf{L10})_3]^{9+}$ and $R_{calc}^{Lu_4(\mathbf{L11})_3} = R_0^{Lu(\mathbf{L11})_3}(1+3\alpha d) = 16.2$ Å for $[Lu_4(\mathbf{L11})_3]^{12+}$ are obtained by applying the 8.23% increase *twice* to the value $R_0^{Lu(\mathbf{L10})_3} = 11.17$ Å and *thrice* to the value $R_0^{Lu(\mathbf{L11})_3} = 12.97$ Å, whilst the experimental values determined from measuring the diffusion coefficients of $[Lu_3(\mathbf{L10})_3]^{9+}$ and $[Lu_4(\mathbf{L11})_3]^{12+}$ are $r_H^{Lu_3(\mathbf{L10})_3} = 11.2(6)$ Å and $r_H^{Lu_4(\mathbf{L11})_3} = 15.6(7)$ Å respectively (Table 4).

Dependence of $\Delta E_{1-x}^{M,M}$ on cation charge: Expressions for the geminal (1-2) and vicinal (1-3) interactions operating between *differently* charged cations, that is $\Delta E_{1-2}^{Zn,Lu}$ and $\Delta E_{1-3}^{Zn,Lu}$, can be obtained by applying a similar analysis to

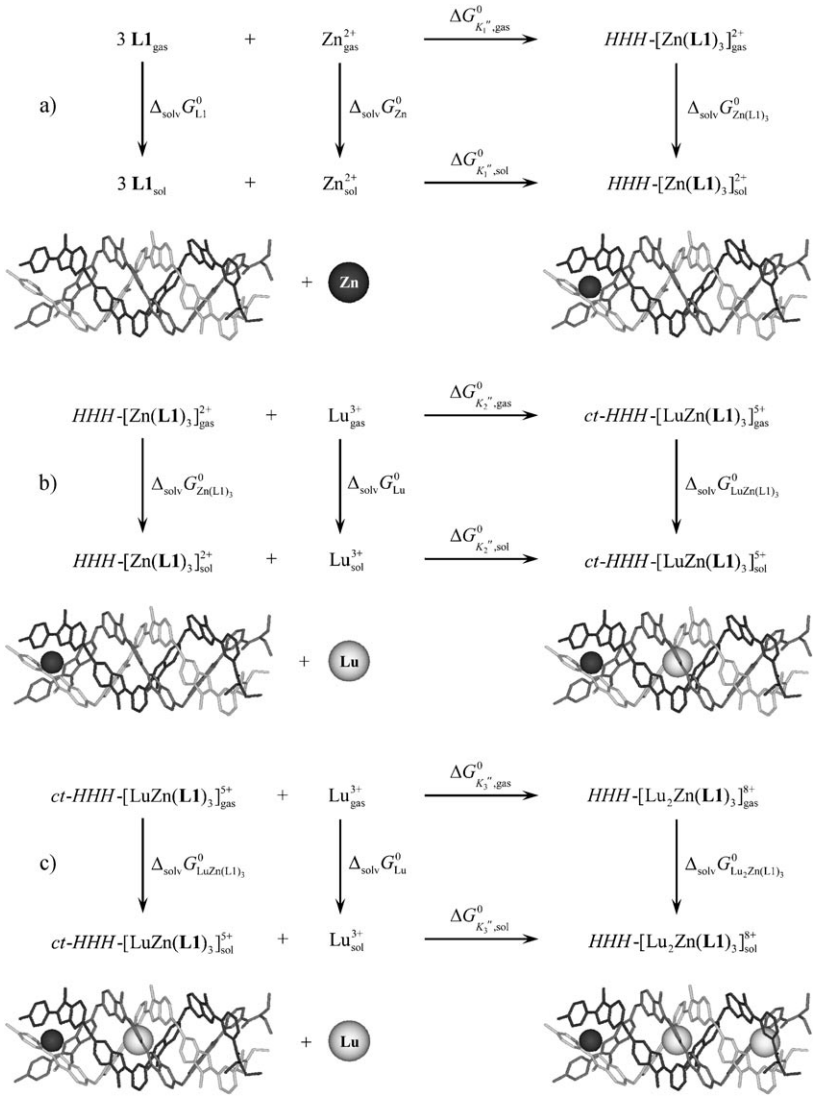

Figure 5. Born–Haber cycles for the successive complexation of a) Zn^{2+} to three strands of **L1** to give *HHH*-$[Zn(\mathbf{L1})_3]^{2+}$, (b) Lu^{3+} to *HHH*-$[Zn(\mathbf{L1})_3]^{2+}$ to give *ct-HHH*-$[LuZn(\mathbf{L1})_3]^{5+}$ and (c) Lu^{3+} to *ct-HHH*-$[LuZn(\mathbf{L1})_3]^{5+}$ to give *HHH*-$[Lu_2Zn(\mathbf{L1})_3]^{8+}$.

that used for Equations (47)–(49) to the three successive complexation reactions leading to the trinuclear bimetallic helicate *HHH*-$[Lu_2Zn(\mathbf{L1})_3]^{8+}$ [Eqs. (51)–(53), Figure 5].

$$3\,\mathbf{L1} + Zn^{2+} \rightleftharpoons \textit{HHH}\text{-}[Zn(\mathbf{L1})_3]^{2+} \quad K_1'' \tag{51}$$

$$\textit{HHH}\text{-}[Zn(\mathbf{L1})_3]^{2+} + Lu^{3+} \rightleftharpoons \textit{ct-HHH}\text{-}[LuZn(\mathbf{L1})_3]^{5+} \quad K_2'' \tag{52}$$

$$\textit{ct-HHH}\text{-}[LuZn(\mathbf{L1})_3]^{5+} + Lu^{3+} \rightleftharpoons \textit{HHH}\text{-}[Lu_2Zn(\mathbf{L1})_3]^{8+} \quad K_3'' \tag{53}$$

A full derivation (see the Supporting Information, Appendix 4) considers the various phase-transfer and complexation processes outlined in the Born–Haber cycles depicted in Figure 5. The final expressions for estimating the intermetallic interactions $\Delta E_{1-2}^{Zn,Lu}$ and $\Delta E_{1-3}^{Zn,Lu}$ in solution are given in Equations (54) and (55).

$$\Delta E_{1-2}^{Zn,Lu} = \frac{e^2 N_A}{4\pi\varepsilon_0}\left(\frac{z_{Zn}z_{Lu}}{d} - \frac{1}{2}\left(1-\frac{1}{\varepsilon_r}\right)\left(-\frac{2(z_{Zn})^2}{R_0^{Zn(\mathbf{L1})_3}} + \frac{(z_{Zn}+z_{Lu})^2}{R_0^{Zn(\mathbf{L1})_3}(1+\alpha d)} - \frac{(z_{Lu})^2}{R_0^{Lu}} + \frac{(z_{Zn})^2}{R_0^{Zn}}\right)\right) + 3\Delta_{solv}G_{\mathbf{L1}}^0 - RT\ln(4) \tag{54}$$

$$\Delta E_{1-3}^{Zn,Lu} = \Delta E_{1-2}^{Zn,Lu} - \Delta E_{1-2}^{Lu,Lu} + \frac{e^2 N_A}{4\pi\varepsilon_0}\left(\frac{(z_{Lu})^2}{d} - \frac{(z_{Lu}z_{Zn})}{2d} - \frac{1}{2R_0^{Zn(\mathbf{L1})_3}}\left(1-\frac{1}{\varepsilon_r}\right)\left(-\frac{2(z_{Lu}+z_{Zn})^2}{(1+\alpha d)} + \frac{(2z_{Lu}+z_{Zn})^2}{(1+2\alpha d)} + (z_{Zn})^2\right)\right) \tag{55}$$

If we assume that the difference in solvation energy between the Zn^{2+} and Lu^{3+} cations in acetonitrile, $\Delta_{solv}G_{Zn}^0 - \Delta_{solv}G_{Lu}^0$, is reasonably approximated by the difference between the corresponding Gibbs free energies of hydration $\Delta_{hyd}G_{Zn}^0 - \Delta_{hyd}G_{Lu}^0 \approx -2040 + 3750 \approx 1710\ kJ\,mol^{-1}$,[44] then the expression $\Delta_{solv}G_{Zn}^0 - \Delta_{solv}G_{Lu}^0 = \frac{e^2N_A}{8\pi\varepsilon_0}\left(\left(1-\frac{1}{\varepsilon_r}\right)\left(\frac{(z_{Lu})^2}{R_0^{Lu}} - \frac{(z_{Zn})^2}{R_0^{Zn}}\right)\right)$ which describes this energy difference in terms of the Born equation can be factored out of Equation (54) and replaced with the former experimental value to give:

$$\Delta E_{1-2}^{Zn,Lu} = \frac{e^2 N_A}{4\pi\varepsilon_0}\left(\frac{z_{Zn}z_{Lu}}{d} - \frac{1}{2}\left(1-\frac{1}{\varepsilon_r}\right)\left(-\frac{2(z_{Zn})^2}{R_0^{Zn(\mathbf{L1})_3}} + \frac{(z_{Zn}+z_{Lu})^2}{R_0^{Zn(\mathbf{L1})_3}(1+\alpha d)}\right)\right) + 3\Delta_{solv}G_{\mathbf{L1}}^0 - RT\ln(4) + 1.71.\times 10^6 \tag{56}$$

In order to validate Equations (55) and (56), we again require knowledge of the effective radius $R_0^{Zn(\mathbf{L1})_3}$ of the tripodal receptor *HHH*-$[Zn(\mathbf{L1})_3]^{2+}$, the expansion factor αd and the solvation energy of **L1**, $\Delta_{solv}G_{\mathbf{L1}}^0$. The first of these can computed in a similar fashion to $R_0^{Lu(\mathbf{L10})_3}$ and $R_0^{Lu(\mathbf{L11})_3}$, by directly applying a 36% increase twice to the value $r_H^{Zn(\mathbf{L2})_3} = 5.33(2)$ Å determined for the complex $[Zn(\mathbf{L2})_3]^{2+}$ from DOSY measurements (Table 4). This gives a value of $R_0^{Zn(\mathbf{L1})_3} \approx r_H^{Zn(\mathbf{L2})_3}(1+2\times0.36) = 9.0$ Å, which may likewise be permitted to vary within the range $8.0 \le R_0^{Zn(\mathbf{L1})_3} \approx 9.0 \le 10.0$ Å. If we then fix the values of $R_0^{Lu(\mathbf{L10})_3} = 11.17$ Å, $R_0^{Lu(\mathbf{L11})_3} = 12.97$ Å and $\alpha d = 8.23\,\%$ obtained above and allow $R_0^{Zn(\mathbf{L1})_3}$ and $\Delta_{solv}G_{\mathbf{L1}}^0$ to vary, exact fits of all five Equations (47)–(49), (55) and (56) to the five intermetallic interactions $\Delta E_{1-x}^{Lu,Lu}$ ($x = 2$–4) and $\Delta E_{1-x}^{Zn,Lu}$ ($x = 2$, 3) listed in Table 1 are obtained when $R_0^{Zn(\mathbf{L1})_3} = 8.90$ Å and $\Delta_{solv}G_{\mathbf{L1}}^0 \approx -490\ kJ\,mol^{-1}$. The optimised effective radius of *HHH*-$[Zn(\mathbf{L1})_3]^{2+}$, $R_0^{Zn(\mathbf{L1})_3} = 8.90$ Å, lies well within the error margin associated with its initial estimate of 9.0 ± 1.0 Å. Likewise, applying the ca. $2\times8.23\,\%$ size increase associated with the successive complexation of two Lu^{3+} trications gives an extrapolated effective radius of $R_{calc}^{Lu_2Zn(\mathbf{L1})_3} \approx r_H^{Zn(\mathbf{L1})_3}(1+2\times0.083) = 10.3$ Å for the ion-saturated complex *HHH*-$[Lu_2Zn(\mathbf{L1})_3]^{8+}$, which is essentially identical to its experimental value of $r_H^{Lu_2Zn(\mathbf{L1})_3} = 10.4(1)$ (Table 4). The adjusted value of $\Delta_{solv}G_{\mathbf{L1}}^0 \approx -490\ kJ\,mol^{-1}$ is less satisfactory, although it does lie within the same order of magnitude as the DFT estimates of $\Delta_{solv}G_{\mathbf{L10}}^0 \approx \Delta_{solv}G_{\mathbf{L1}}^0 \approx -200$ to $-270\ kJ\,mol^{-1}$. It is also worth noting that, whilst the solvation energy of **L10** was underestimated by ca. $100\ kJ\,mol^{-1}$ with respect to DFT methods, that of **L1** is over estimated by about $250\ kJ\,mol^{-1}$. This discrepancy reflects the limitation of our approximate electrostatic model, combined with the assumption that the non-constrained effective radii required by the Born equation are assigned to the hydrodynamic radii measured in acetonitrile solution.

Conclusions

Application of the site binding model to the cumulative stability constants of some 29 mono- and polynuclear triple-helical complexes of Lu^{3+} and Zn^{2+} succeeds in the estimation of a minimum set of ten microscopic thermodynamic descriptors, which satisfyingly reproduce the global experimental data. As expected, intermolecular metal–ligand connections (including desolvation) provide the favorable driving force responsible for the formation of the final self-assembled complexes. These are, however, systematically destabilised by i) the mediocre preorganisation of the ligand strands for intramolecular (macro)cyclization and ii) some minor short-range interligand and intermetallic interactions (anti-cooperative effects). Focusing on the anomalously weak intermetallic interactions in solution and on their counter-intuitive dependence on intermetallic separation ($\Delta E_{1-4}^{Ln,Lu} > \Delta E_{1-2}^{Ln,Lu}$ and $\Delta E_{1-3}^{Ln,Lu} < 0$) and cationic charges ($\Delta E_{1-2}^{Zn,Lu} > \Delta E_{1-2}^{Ln,Lu}$) brings

to light the competition between familiar electrostatic repulsions and often neglected stabilizing solvation effects, which result from the increase of the total charge of the polynuclear complexes. The main lesson for coordination chemists concerns the rational design of stable and highly charged polynuclear complexes in polar solution, which indeed mainly results from a judicious control of the molecular shape maximizing favorable solvation energies. By chance, the empirical design of the semi-rigid segmental ligands **L1**–**L11** produces a geminal intermetallic separation of about 9 Å in the triple-helical complexes, for which the intermetallic Coulomb repulsion is almost exactly overcome by the increase in solvation energy due the larger charge borne by the helicate. We are, however, now equipped for predicting and programming (by ligand design) the operation of either strongly negatively (i.e. anti-cooperative) or positively cooperative complexation processes in one-dimensional helicates. For instance, if all the structural parameters characterizing the assembly of $[Lu_3(\mathbf{L10})_3]^{9+}$ and $[Lu_4(\mathbf{L11})_3]^{12+}$ are maintained at their fitted values ($R_0^{Lu(\mathbf{L10})_3}=11.17$ Å, $R_0^{Lu(\mathbf{L11})_3}=12.97$ Å and $\Delta_{solv}G^0_{\mathbf{L10}}=-150\,kJ\,mol^{-1}$), whilst the rigidity of the triple-helical scaffold is slightly increased from $\alpha d=8.23\,\%$ to $\alpha d=5\,\%$ (for example, by limiting the degrees of freedom of the methylene linkers), we anticipate the operation of highly cooperative self-assembly processes with $\Delta E^{Ln,Lu}_{1-2}=-58\,kJ\,mol^{-1}$, $\Delta E^{Ln,Lu}_{1-3}=-145\,kJ\,mol^{-1}$ and $\Delta E^{Ln,Lu}_{1-4}=-148\,kJ\,mol^{-1}$. On the contrary, the preservation of the same moderate rigidity ($\alpha d=8.23\,\%$), but modulated with a reduction in the intermetallic separation from $d=9$ Å to 7 Å, and a concomitant decrease of (1-7/9)·100=22 % in the effective radii ($R_0^{Lu(\mathbf{L10})_3}=9$ Å, $R_0^{Lu(\mathbf{L11})_3}=10$ Å), results in strongly anti-cooperative behaviour, with $\Delta E^{Ln,Lu}_{1-2}=178\,kJ\,mol^{-1}$, $\Delta E^{Ln,Lu}_{1-3}=21\,kJ\,mol^{-1}$ and $\Delta E^{Ln,Lu}_{1-4}=18\,kJ\,mol^{-1}$. The same type of predictive calculation can be performed upon modification of the charge of the entering cations. We compute, for instance, that the replacement of Lu^{3+} in *HHH*-$[Lu_2Zn(\mathbf{L1})_3]^{8+}$, $[Lu_3(\mathbf{L10})_3]^{9+}$ and $[Lu_4(\mathbf{L11})_3]^{12+}$ by Ca^{2+} in the related *HHH*-$[Ca_2Zn(\mathbf{L1})_3]^{6+}$, $[Ca_3(\mathbf{L10})_3]^{6+}$ and $[Ca_4(\mathbf{L11})_3]^{8+}$ complexes, all other parameters being fixed to their values estimated for the Lu/Zn system, gives rise to a positively cooperative process with $\Delta E^{Ca,Ca}_{1-2}=-255\,kJ\,mol^{-1}$, $\Delta E^{Ca,Ca}_{1-3}=-4\,kJ\,mol^{-1}$, $\Delta E^{Ca,Ca}_{1-4}=8\,kJ\,mol^{-1}$, $\Delta E^{Ca,Zn}_{1-2}=-90\,kJ\,mol^{-1}$ and $\Delta E^{Ca,Zn}_{1-3}=-74\,kJ\,mol^{-1}$. Although the simple point charge electrostatic model proposed limits the accuracy of the absolute values found for the apparent intermetallic interactions in solution, it provides coordination chemists with some valuable clues for the design of related one-dimensional complexes with predetermined thermodynamic properties in solution. Obviously, this approach can also be adapted for two- and three-dimensional complexes in which perhaps even more counter-intuitive effects are envisaged as a result of i) a more elaborate network of through-space intermetallic interactions and ii) more subtle changes in molecular size and shape incurred on sequential increases in nuclearity.

Experimental Section

DFT calculation of solvation energies: Density functional theory (DFT) calculations were performed to estimate the solvation energies of ligands **L1** and **L10** as well as the difference between the solvation energies of Zn^{2+} and Lu^{3+} in acetonitrile. The TURBOMOLE 5.10 package was employed.[45] The BP86 exchange correlation functional[46] was used along with triple-zeta valence plus polarization (TZVP) basis sets on all atoms.[47,48] A quasirelativistic pseudopotential was used for the lutetium atom with 28 core electrons. To speed up the calculations, the Coulomb part was evaluated by using the MARI-J method[49,50] along with optimised TZVP auxiliary basis sets on all atoms.[51] The conductor-like screening model (COSMO)[52,53] was employed to describe the solvent. Solvation free energies of the ligands were also obtained using the SM8 solvation model[54] as implemented in MN-GSM,[55] a locally modified version of the Gaussian03 package.[56] These calculations were performed with the M06 L functional[57] in combination with the 6-31G(d) basis set[58] on all atoms. The difference in the solvation energies of Zn^{2+} and Lu^{3+} ($\Delta_{solv}G^0_{Zn}-\Delta_{solv}G^0_{Lu}\approx1640\,kJ\,mol^{-1}$) was computed as follows: The formation energies of the $[Zn(MeCN)_6]^{2+}$ ($\Delta_{solv}G^0_{Zn(MeCN)_6}=-1717\,kJ\,mol^{-1}$) and $[Lu(MeCN)_9]^{3+}$ ($\Delta_{solv}G^0_{Lu(MeCN)_9}=-2834\,kJ\,mol^{-1}$) complexes in the gas-phase (i.e. $Zn^{2+}+6\,MeCN\rightarrow[Zn(MeCN)_6]^{2+}$ and $Lu^{3+}+9\,MeCN\rightarrow[Lu(MeCN)_9]^{3+}$, respectively) were determined as an estimate of the inner-sphere contribution to solvation. The solvation energies of the solvate complexes ($\Delta_{solv}G^0_{Zn(MeCN)_6}=-525\,kJ\,mol^{-1}$ and $\Delta_{solv}G^0_{Lu(MeCN)_9}=-1046\,kJ\,mol^{-1}$) were then calculated as for ligands **L1** and **L10** and added to the complex formation energies as an estimate of the outer-sphere contribution to solvation. The difference in solvation energy between Zn^{2+} and Lu^{3+} thus corresponds to $\Delta_{solv}G^0_{Zn}-\Delta_{solv}G^0_{Lu}\approx(\Delta G^0_{Zn(MeCN)_6}+\Delta_{solv}G^0_{Zn(MeCN)_6})-(\Delta G^0_{Lu(MeCN)_9}+\Delta_{solv}G^0_{Lu(MeCN)_9})\approx1640\,kJ\,mol^{-1}$.

Syntheses and spectroscopic measurements: Chemicals were purchased from Fluka AG and Aldrich, and used without further purification unless otherwise stated. The ligands **L1**,[24] **L2**,[25] **L3**,[26] **L4**,[27] **L5**,[28] **L6**,[29] **L7**,[30] **L8**,[22,31] **L9**,[32] **L10**[33] and **L11**,[21] and their complexes were prepared according to literature procedures. The trifluoromethanesulfonate salt $Lu(CF_3SO_3)_3{\cdot}x\,H_2O$ was prepared from the corresponding oxide (Aldrich, 99.99 %).[59] The Lu content of solid salt was determined by complexometric titrations with Titriplex III (Merck) in the presence of urotropine and xylene orange.[60] Acetonitrile was distilled over calcium hydride. Pneumatically-assisted electrospray (ESI-MS) mass spectra were recorded from 10^{-4} M solutions on a Finnigan SSQ7000 instrument. Diffusion experiments (DOSY-NMR) were carried out at 400 MHz-Larmor frequency (293 K, $|complex|_{tot}=5\times10^{-3}$ M). The complexes were prepared in situ and left to equilibrate for 48 h (CD_3CN, 293 K, $|complex|_{tot}=5\times10^{-3}$ M). The pulse sequence used was the Bruker pulse program *ledbpgp2s*[61] which employs stimulated echo, bipolar gradients and longitudinal eddy current delay as the z filter. The four 2 ms gradient pulses have sine-bell shapes and amplitudes ranging linearly from 2.5 to 50 G cm^{-1} in 32 steps. The diffusion delay was in the range 60–140 ms depending on the analyte diffusion coefficient, and the no. of scans was 32. The processing was done using a line broadening of 5 Hz and the diffusion coefficients were calculated with the Bruker processing package. Least-square fits were performed with Excel, Mathematica and Matlab.

Acknowledgements

We thank C. J. Cramer for help in setting up SM8 calculations. Financial support from the Swiss National Science Foundation, from the European Commission "Directorate D—The human factor, mobility, and Marie-Curie activities" framework and from the Swiss Office for Science and Education within the frame of the ESF COST Action D31 are gratefully acknowledged.

[1] a) M. Mammen, S.-K. Choi, G. M. Whitesides, *Angew. Chem.* **1998**, *110*, 2908–2953; *Angew. Chem. Int. Ed.* 1998, 37, 2754–2794; b) V. M. Krishnamurthy, B. R. Bohall, V. Semetey, G. M. Whitesides, *J. Am. Chem. Soc.* 2006, 128, 5802–5812.
[2] a) W. T. S. Huck, N. Bowden, P. Onck, T. Pardoen, J. W. Hutchinson, G. M. Whitesides, *Langmuir* **2000**, *16*, 3497–3501; b) V.-R. Thalladi, A. Schwartz, J. N. Phend, J. W. Hutchinson, G. M. Whitesides, *J. Am. Chem. Soc.* **2002**, *124*, 9412–9417.
[3] J.-M. Lehn, *Angew. Chem.* **1988**, *100*, 91–116; *Angew. Chem. Int. Ed. Engl.* **1988**, *27*, 89–112.
[4] a) J.-M. Lehn, *Supramolecular Chemistry*, VCH, Weinheim, **1995**; b) D. Philp, J. F. Stoddart, *Angew. Chem.* **1996**, *108*, 1242–1286; *Angew. Chem. Int. Ed. Engl.* **1996**, *35*, 1154–1196; c) V. Balzani, A. Credi, M. Venturi, *Chem. Eur. J.* **2002**, 8, 5525–5532; d) J.-M. Lehn, *Chem. Soc. Rev.* **2007**, *36*, 151–160; e) V. Balzani, A. Credi, M. Venturi, *Chem. Eur. J.* **2008**, *14*, 26–39; f) J. W. Steed, J. L. Atwood, *Supramolecular Chemistry*, 2nd ed., Wiley, Chichester, **2009**.
[5] a) C. Piguet, G. Bernardinelli, G. Hopfgartner, *Chem. Rev.* **1997**, *97*, 2005–2062; b) B. Olenyuk, A. Fechtenkötter, P. J. Stang, *J. Chem. Soc. Dalton Trans.* **1998**, 1707–1728; c) F. M. Raymo, J. F. Stoddart, *Curr. Opin. Colloid Interface Sci.* **1998**, *3*, 150–159; d) S. Leininger, B. Olenyuk, P. J. Stang, *Chem. Rev.* **2000**, *100*, 853–907; e) A. Mulder, J. Huskens, D. N. Reinhoudt, *Org. Biomol. Chem.* **2004**, *2*, 3409–3424; f) J. D. Badjic, A. Nelson, S. J. Cantrill, W. B. Turnbull, J. F. Stoddart, *Acc. Chem. Res.* **2005**, *38*, 723–732; g) G. V. Oshovsky, D. N. Reinhoudt, W. Verboom, *Angew. Chem.* **2007**, *119*, 2418–2445; *Angew. Chem. Int. Ed.* **2007**, *46*, 2366–2393; h) L. Zhao, B. H. Northrop, P. J. Stang, *J. Am. Chem. Soc.* **2008**, *130*, 11886–11888.
[6] a) G. Ercolani, *J. Am. Chem. Soc.* **2003**, *125*, 16097–16103; b) G. Ercolani, *J. Phys. Chem. B* **2003**, *107*, 5052–5057.
[7] J.-M. Senegas, S. Koeller, C. Piguet, *Chem. Commun.* **2005**, 2235–2237.
[8] G. Ercolani, C. Piguet, M. Borkovec, J. Hamacek, *J. Phys. Chem. B* **2007**, *111*, 12195–12203.
[9] a) R. Krämer, J.-M. Lehn, A. Marquis-Rigault, *Proc. Natl Acad. Sci. USA* 1993, 90, 5394–5398; b) J.-M. Lehn, A. V. Eliseev, *Science* **2001**, *291*, 2331–2333; c) J. Hamacek, M. Borkovec, C. Piguet, *Chem. Eur. J.* **2005**, *11*, 5217–5226; d) J. Hamacek, M. Borkovec, C. Piguet, *Chem. Eur. J.* **2005**, *11*, 5227–5237.
[10] D. Munro, *Chem. Br.* 1977, 13, 100–105.
[11] a) W. Kuhn, *Kolloid-Z.* **1934**, 68, 2–15; b) H. Jacobson, W. H. Stockmayer, *J. Chem. Phys.* **1950**, *18*, 1600–1606; c) P. J. Flory, U. W. Suter, M. Mutter, *J. Am. Chem. Soc.* **1976**, *98*, 5733–5739; d) W. P. Jencks, *Proc. Natl. Acad. Sci. USA* **1981**, *78*, 4046–4050; e) M. Winnik, *Chem. Rev.* **1981**, *81*, 491–524; f) J. M. Gargano, T. Ngo, J. Y. Kim, D. W. K. Acheson, W. J. Lees, *J. Am. Chem. Soc.* **2001**, *123*, 12909–12910; g) R. H. Kramer, J. W. Karpen, *Nature* **1998**, *395*, 710–713; h) P. I. Kitov, D. R. Bundle, *J. Am. Chem. Soc.* **2003**, *125*, 16271–16284; i) G. Ercolani, *Struct. Bonding (Berlin)* 2006, 121, 167–215; j) C. Hunter, S. Tomas, *J. Am. Chem. Soc.* **2006**, *128*, 8975–8979; k) T. M. Fyles, C. C. Tong, *New J. Chem.* **2007**, *31*, 296–304; l) V. M. Krishnamurthy, V. Semetey, P. J. Bracher, N. Shen, G. M. Whitesides, *J. Am. Chem. Soc.* **2007**, *129*, 1312–1320.
[12] a) D. L. Caulder, K. N. Raymond, *J. Chem. Soc. Dalton Trans.* **1999**, 1185–1200; b) D. L. Caulder, K. N. Raymond, *Acc. Chem. Res.* **1999**, *32*, 975–982; c) M. D. Levin, P. J. Stang, *J. Am. Chem. Soc.* **2000**, *122*, 7428–7429.
[13] a) P. J. Stang, B. Olenyuk, *Acc. Chem. Res.* **1997**, *30*, 502–518; b) E. Chekmeneva, C. A. Hunter, M. J. Packer, S. M. Turega, *J. Am. Chem. Soc.* **2008**, *130*, 17718–17725.
[14] J. Hamacek, M. Borkovec, C. Piguet, *Dalton Trans.* **2006**, 1473–1490.
[15] B. Perlmutter-Hayman, *Acc. Chem. Res.* **1986**, *19*, 90–96.
[16] J. Hamacek, C. Piguet, *J. Phys. Chem. B* **2006**, *110*, 7783–7792.
[17] M. Borkovec, G. J. M. Koper, C. Piguet, *Curr. Opin. Colloid Interface Sci.* 2006, 11, 280–289.
[18] G. Koper, M. Borkovec, *J. Phys. Chem. B* **2001**, *105*, 6666–6674.
[19] C. Piguet, M. Borkovec, J. Hamacek, K. Zeckert, *Coord. Chem. Rev.* **2005**, *249*, 705–726.
[20] a) A. Pfeil, J.-M. Lehn, *J. Chem. Soc. Chem. Commun.* **1992**, 838–839; b) N. Fatin-Rouge, S. Blanc, A. Pfeil, A. Rigault, A.-M. Albrecht-Gary, J.-M. Lehn, *Helv. Chim. Acta* **2001**, *84*, 1694–1711.
[21] N. Dalla Favera, J. Hamacek, M. Borkovec, D. Jeannerat, F. Gumy, J.-C. G. Bünzli, G. Ercolani, C. Piguet, *Chem. Eur. J.* **2008**, *14*, 2994–3005.
[22] G. Canard, C. Piguet, *Inorg. Chem.* **2007**, *46*, 3511–3522.
[23] a) M. Born, *Z. Phys.* **1920**, *1*, 45–48; b) R. H. Stokes, *J. Phys. Chem.* **1964**, *68*, 979–982; c) T. Abe, *Bull. Chem. Soc. Jpn.* 1991, 64, 3035–3038; d) B. E. Conway in *Modern Aspects of Electrochemistry* (Eds.: B. E. Conway, R. E. White), Kluwer, **2002**, pp. 295–323.
[24] T. Riis-Johannessen, G. Bernardinelli, Y. Filinchuk, S. Clifford N. Dalla Favera, C. Piguet, *Inorg. Chem.* **2009**, *48*, 5512–5525.
[25] a) L. J. Charbonnière, A. F. Williams, C. Piguet, G. Bernardinelli, E. Rivera-Minten, *Chem. Eur. J.* **1998**, *4*, 485; b) S. Torelli, S. Delahaye, A. Hauser, G. Bernardinelli, C. Piguet, *Chem. Eur. J.* **2004**, *10*, 3503–3516.
[26] S. Petoud, J.-C. G. Bünzli, F. Renaud, C. Piguet, K. J. Schenk, G. Hopfgartner, *Inorg. Chem.* **1997**, *36*, 5750–5760.
[27] T. Le Borgne, P. Altmann, N. André, J.-C. G. Bünzli, G. Bernardinelli, P.-Y. Morgantini, J. Weber, C. Piguet, *Dalton Trans.* **2004**, 723–733.
[28] K. Zeckert, J. Hamacek, J.-P. Rivera, S. Floquet, A. Pinto, M. Borkovec, C. Piguet, *J. Am. Chem. Soc.* **2004**, *126*, 11589–11601.
[29] J. Hamacek, S. Blanc, M. Elhabiri, E. Leize, A. Van Dorsselaer, C. Piguet, A.-M. Albrecht-Gary, *J. Am. Chem. Soc.* **2003**, *125*, 1541–1550.
[30] a) N. André, T. B. Jensen, R. Scopelliti, D. Imbert, M. Elhabiri, G. Hopfgartner, C. Piguet, J.-C. G. Bünzli, *Inorg. Chem.* **2004**, *43*, 515–529; b) N. André, R. Scopelliti, G. Hopfgartner, C. Piguet, J.-C. G. Bünzli, *Chem. Commun.* **2002**, 214–216.
[31] C. Piguet, J.-C. G. Bünzli, G. Bernardinelli, G. Hopfgartner, S. Petoud, O Schaad, *J. Am. Chem. Soc.* **1996**, *118*, 6681–6697.
[32] C. Piguet, E. Rivara-Minten, G. Hopfgartner, J.-C. G. Bünzli, *Helv. Chim. Acta* **1995**, *78*, 1541–1566.
[33] S. Floquet, N. Ouali, B. Bocquet, G. Bernardinelli, D. Imbert, J.-C. G. Bünzli, G. Hopfgartner, C. Piguet, *Chem. Eur. J.* **2003**, *9*, 1860–1875.
[34] S. W. Benson, *J. Am. Chem. Soc.* 1958, 80, 5151–5154.
[35] To simplify the calculation of symmetry numbers we have considered the solvated Lu^{3+} ion as a nine-coordinate tricapped trigonal prismatic complex of D_{3h} symmetry. Statistical factors have also been calculated by considering an eight coordinate square antiprism for Lu^{3+}, but exchanging one set of factors for another has no influence whatsoever on the adjusted values obtained from subsequent regression analyses (see next section).
[36] G. Canard, S. Koeller, G. Bernardinelli, C. Piguet, *J. Am. Chem. Soc.* **2008**, *130*, 1025–1040.
[37] 18 Å corresponds to a generous estimate of the maximum possible distance separating two adjacent binding sites of a segmental ligand, such as **L1** and **L5**–**L11** prior to an intramolecular closure (in one of their corresponding polymetallic complexes).
[38] S. L. Cockroft, C. A. Hunter, K. R. Lawson, J. Perkins, C. J. Urch, *J. Am. Chem. Soc.* **2005**, *127*, 8594–8595.
[39] a) F. Berny, N. Muzet, L. Troxler, A. Dedieu, G. Wipff, *Inorg. Chem.* 1999, 38, 12441252; b) M. Baaden, F. Berny, C. Madic, G. Wipff, *J. Phys. Chem. A* 2000, 104, 7659–7671; c) G. Wipff, F. Berny, *J. Chem. Soc. Perkin Trans. 2* 2001, 73–82.
[40] c = central and t = terminal correspond to the locations of the Lu^{3+} ions in the central N_9 and terminal N_6O_3 binding cavities of three co-aligned strands of **L10**. If not specified in the prefix, a *HHH*-alignment of ligands is assumed for all structures, as shown in Figure 4.
[41] A. Macchioni, G. Ciancaleoni, C. Zuccaccia, D. Zuccaccia, *Chem. Soc. Rev.* **2008**, *37*, 479–489, and references therein.

[42] a) A. Einstein, *Ann. Phys.* 1906, 19, 289–306; b) A. Einstein, *Ann. Phys.* 1906, 19, 371–381; c) M. Sharma, S. Yashonath, *J. Phys. Chem. B* **2006**, *110*, 17207–17211.
[43] a) A. Gierer, K. Wirtz, *Z. Naturforsch. A* 1953, 8, 532–538; b) H.-C. Chen, S.-H. Chen, *J. Phys. Chem.* **1984**, *88*, 5118–5121.
[44] a) J. Burgess, *Metal Ions in Solution*, EllisHorwood, Chichester, **1978**, pp. 182–190. b) We have also computed this value by DFT to be about 1640 kJ mol^{-1} (see Experimental Section).
[45] R. Ahlrichs, M. Baer, M. Haeser, H. Horn, C. Koelmel, *Chem. Phys. Lett.* **1989**, *162*, 165–169.
[46] J. P. Perdew, *Phys. Rev. B* **1986**, *33*, 8822–8824.
[47] F. Weigend, R. Ahlrichs, *Phys. Chem. Chem. Phys.* **2005**, *7*, 32973305.
[48] K. Eichkorn, F. Weigend, O. Treutler, R. Ahlrichs, *Theor. Chem. Acc.* **1997**, *97*, 119–124.
[49] K. Eichkorn, O. Treutler, H. Uhm, M. Häser, R. Ahlrichs, *Chem. Phys. Lett.* **1995**, *242*, 652–660.
[50] M. Sierka, A. Hogekamp, R. Ahlrichs, *J. Chem. Phys.* **2003**, *118*, 9136–9148.
[51] F. Weigend, *Phys. Chem. Chem. Phys.* **2006**, *8*, 1057–1065.
[52] A. Klamt, G. Schüürmann, *J. Chem. Soc. Perkin Trans. 2* **1993**, 799–805.
[53] G. Schäfer, A. Klamt, D. Sattel, J. C. W. Lohrenz, F. Eckert, *Phys. Chem. Chem. Phys.* **2000**, *2*, 2187–2193.
[54] A. V. Marenich, R. M. Olson, C. P. Kelly, C. J. Cramer, D. G. Truhlar, *J. Chem. Theory Comput.* **2007**, *3*, 2011–2033.
[55] R. M. Olson, A. V.; Marenich, A. C. Chamberlin, C. P. Kelly, J. D. Xidos, J. Li, J. D. Thompson, G. D. Hawkins, P. D. Winget, T. Zhu, D. Rinaldi, D. A. Liotard, C. J. Cramer, D. G. Truhlar, M. J. Frisch, *MN-GSM version 2008*, University of Minnesota: Minneapolis, **2008**.
[56] M. J. Frisch, G. W. Trucks, H. B. Schlegel, G. E. Scuseria, M. A. Robb, J. R. Cheeseman, J. A. Montgomery, T. Vreven, K. N. Kudin, J. C. Burant, J. M. Millam, S. S. Iyengar, J. Tomasi, V. Barone, B. Mennucci, M. Cossi, G. Scalmani, N. Rega, G. A. Petersson, H. Nakatsuji, M. Hada, M. Ehara, K. Toyota, R. Fukuda, J. Hasegawa, M. Ishida, T. Nakajima, Y. Honda, O. Kitao, H. Nakai, M. Klene, X. Li, J. E. Knox, H. P. Hratchian, J. B. Cross, C. Adamo, J. Jaramillo, R. Gomperts, R. E. Stratmann, O. Yazyev, A. J. Austin, R. Cammi, C. Pomelli, J. W. Ochterski, P. Y. Ayala, K. Morokuma, G. A. Voth, P. Salvador, J. J. Dannenberg, V. G. Zakrzewski, S. Dapprich, A. D. Daniels, M. C. Strain, O. Farkas, D. K. Malick, A. D. Rabuck, K. Raghavachari, J. B. Foresman, J.-V. Ortiz, Q. Cui, A. G. Baboul, S. Clifford, J. Cioslowski, B. B. Stefanov, G. Liu, A. Liashenko, P. Piskorz, I. Komaromi, R. L. Martin, D. J. Fox, T. Keith, M. A. Al-Laham, C. Y. Peng, A. Nanayakkara, M. Challacombe, P. M. W. Gill, B. Johnson, W. Chen, M. W. Wong, C. Gonzalez, J. A. Pople, Gaussian03; Gaussian, Inc.: Pittsburgh, PA, **2003**.
[57] Y. Zhao, D. G. Truhlar, *J. Chem. Phys.* 2006, 125, 194101.
[58] M. J. Hehre, L. Radom, P. V. R Schleyer, J. A. Pople, *Ab Initio Molecular Orbital Theory*, Wiley, New York, **1986**.
[59] J. F. Desreux in *Lanthanide Probes in Life, Chemical and Earth Sciences* (Eds.: J.-C. G. Bünzli, G. R. Choppin), Elsevier, Amsterdam, **1989**, chap. 2.
[60] G. Schwarzenbach, *Complexometirc Titrations*, Chapman and Hall, London, **1957**, p. 8.
[61] D. Wu, A. Chen, C. S. Jr Johnson, *J. Magn. Reson. Ser. A* **1995**, *115*, 260–264.

Received: April 6, 2009
Published online: October 20, 2009

